

GROWTH MODEL FOR ABDOMINAL AORTIC ANEURYSMS USING  
LONGITUDINAL CT IMAGES

A THESIS SUBMITTED TO  
THE GRADUATE SCHOOL OF INFORMATICS OF  
MIDDLE EAST TECHNICAL UNIVERSITY

BY

EMRAH AKKOYUN

IN PARTIAL FULFILLMENT OF THE REQUIREMENTS FOR THE DEGREE  
OF  
DOCTOR OF PHILOSOPHY  
IN  
MEDICAL INFORMATICS

MARCH 2019



Approval of the thesis:

**GROWTH MODEL FOR ABDOMINAL AORTIC ANEURYSMS USING  
LONGITUDINAL CT IMAGES**

submitted by **EMRAH AKKOYUN** in partial fulfillment of the requirements for the degree of **Doctor of Philosophy in Health Informatics Department, Middle East Technical University** by,

Prof. Dr. Deniz Zeyrek Bozsahin  
Dean, **Graduate School of Informatics**

\_\_\_\_\_

Assoc. Prof. Dr. Yeşim Aydın Son  
Head of Department, **Health Informatics**

\_\_\_\_\_

Assist. Prof. Dr. Aybar Can Acar  
Supervisor, **Health Informatics Dept., METU**

\_\_\_\_\_

Assoc. Prof. Dr. Seungik Baek  
Co-Supervisor, **Mechanical Engineering Dept.,  
Michigan State University**

\_\_\_\_\_

**Examining Committee Members:**

Prof. Dr. Tolga CAN  
Computer Engineering Dept., METU

\_\_\_\_\_

Assist. Prof. Dr. Aybar Can Acar  
Health Informatics Dept., METU

\_\_\_\_\_

Assoc. Prof. Dr. Yeşim Aydın SON  
Health Informatics Dept., METU

\_\_\_\_\_

Assoc. Prof. Dr. Mehmet TAN  
Computer Engineering Dept., TOBB University of  
Economics and Technology

\_\_\_\_\_

Prof. Dr. İlkan TATAR  
Anatomy Dept., Hacettepe University

\_\_\_\_\_

**Date: 02.03.2020**



**I hereby declare that all information in this document has been obtained and presented in accordance with academic rules and ethical conduct. I also declare that, as required by these rules and conduct, I have fully cited and referenced all material and results that are not original to this work.**

**Name, Last name : Emrah AKKOYUN**

**Signature : \_\_\_\_\_**

## **ABSTRACT**

### **GROWTH MODEL FOR ABDOMINAL AORTIC ANEURYSMS USING LONGITUDINAL CT IMAGES**

AKKOYUN, Emrah

Ph.D., Department of Health Informatics

Supervisor: Assist. Prof. Dr. Aybar Can ACAR

Co-Supervisor: Assoc. Prof. Dr. Seungik BAEK

March 2020, 74 pages

An Abdominal Aortic Aneurysm (AAA) is diagnosed by an enlargement of the abdominal aorta. The rupture of an AAA, associated with high mortality, is eventually observed if no surgical intervention is performed. Aneurysm repair prior to rupture is thus vital. The decision to intervene is made primarily based on the AAA size measured by a maximum diameter or its growth rate. However, 10 – 24% of aneurysms below the intervention threshold experience rupture in some series. There are many complex interactions involved, from the hemodynamics and geometric properties of the aorta to patient demographic information, affecting the aneurysms' expansion. Furthermore, the follow-up diameters can be predictable if a patient follows the common growth model of the population. However, a rapid expansion of AAA, often associated with higher rupture risk, might be observed. This study aims to build enhanced Bayesian inference methods to predict maximum aneurysm diameter using 106 CT scans. The utility of master curves and their prediction capabilities in terms of different geometrical parameters were examined. Among all the parameters, the master curve of spherical diameter performed best, predicting the diameter within 0.42 mm in 95% of all scans. Furthermore, a two-step approach based on Bayesian calibration was used and the aneurysm growth model was specified according to individual patient characteristics. Using the enhanced prediction model, 86% of scans were correctly predicted. Thus, the prediction of a measurement at any time-point can be made, along with an associated uncertainty to provide a clinically helpful tool for surgical planning and patient management.

**Keywords:** Abdominal aortic aneurysm, clinical decision making, aneurysm growth, probabilistic programming, patient-oriented growth modeling

## ÖZ

### ABDOMİNAL AORT ANEVİZMALARINDA BOYLAMSAL VERİ KULLANILARAK BÜYÜMENİN MODELLENMESİ

AKKOYUN, Emrah

Doktora, Tıp Bilişimi Bölümü

Tez Danışmanı: Dr. Öğr. Üyesi Aybar Can ACAR

Yardımcı Tez Danışmanı: Doç. Dr. Seungik BAEK

Mart 2020, 74 sayfa

Abdominal Aort Anevrizması (AAA), aort damarının genişlemesi olarak tanımlanır. Herhangi bir cerrahi müdahale yapılmadığında, nihayetinde %80'den fazla bir oranda ölümle sonuçlanan AAA yırtılması gözlemlenir. Bu nedenle yırtılmadan önce anevrizmanın tamiri hayatidir. Müdahale kararı, anevrizmanın maksimum çapına veya yıllık büyüme oranlarına bakılarak verilir. Buna rağmen, anevrizmaların %10 ile %24'ünde belirlenen maksimum sınır değerlerinin altında yırtılma olmaktadır. Hemodinamik ve aortun geometrik özelliklerinden hastanın demografik bilgisine kadar pek çok karmaşık etkileşim, anevrizmanın büyümesini etkilemektedir. Bunun yanında, eğer hasta popülasyona ait ortak büyüme modelini takip ederse, bir sonraki anevrizma çapı tahmin edilebilir. Ancak, yüksek yırtılma riskine sahip hızlı büyüyen AAA'lar gözlemlenebilmektedir. Bu çalışma, 106 BT görüntüsü kullanarak maksimum anevrizma çapının Bayes çıkarsama aracılığıyla tahmin etmeyi amaçlamaktadır. Temel eğrinin faydası ve bu eğrilerin farklı geometrik özelliklerle tahmin edebilme yeteneğini sorgulandı. Bu parametreler arasından en büyük çap ile oluşturulan temel eğri, 0.42 mm hata payı ile tüm görüntülerin %95'ini doğru tahmin ederek en iyi performansı sergilemiştir. Ayrıca, iki aşamalı Bayesian kalibrasyonu kullanılmış ve anevrizma büyüme modeli her bir hastanın karakteristiğine uygun oluşturulmuştur. Anevrizmaların %86'sı geliştirilmiş tahminleme modeli ile tahmin edilmiştir. Böylece, cerrahi planlama ve hastaların yönetimi için klinik olarak yararlı bir araç sunmak amacıyla, herhangi bir zaman noktasında güven aralığı verilerek ölçümün tahmin edilmesi yapılabilmektedir.

**Anahtar Sözcükler:** Abdominal aort anevrizması, klinik karar verme, anevrizma büyümesi, olasılıksal programlama, hastaya özgü büyümenin modellenme

*To my lovely children,  
Ali'm and Ayşe'm*



## ACKNOWLEDGEMENTS

There are many people that have earned my gratitude for their contribution to my time in graduate school. Without their precious support it would not be possible to conduct this research.

First, I wish to express my sincere appreciation to my supervisor, Dr. Aybar C. Acar, who has the substance of a genius: he convincingly guided and encouraged me to be professional and do the right thing even when the road got tough.

I am greatly appreciative of my co-advisor Dr. Seungik Baek, without whom I would not have made it through my PhD degree. The meetings and conversations were vital in inspiring me to think outside the box, from multiple perspectives to form a comprehensive and objective critique.

Besides my advisors, I am grateful to the members of thesis examining committee for their extensive personal and professional guidance, and insightful comments.

I am thankful to all the research group members at Michigan State University, especially to my friends Dr. Hamid and Dr. Byron, whose insight and knowledge into the subject matter steered me through this research.

I would like to give special thanks to my colleagues Onur Bektaş, Ömer Faruk Çangır and my friends, Mustafa Işık, Emel Geçsek, Kenan Koç, Bilge Böğür, Maureen Toppel and Judith Andre for their continued support and encouragement.

Last but not least, I would like to express my deepest gratitude to my lovely children, Ali Tuna and Ayşe Naz, who provide unending inspiration, to my siblings, Feride Yıldırım, Fatih Akkoyun and Nuran Varol, and to my parents for all the support they have shown me through this research. This dissertation would not have been possible without their warm love, continued patience, and endless support.

## TABLE OF CONTENTS

ABSTRACT .....	iv
ÖZ .....	v
DEDICATION.....	vi
ACKNOWLEDGEMENTS .....	vii
TABLE OF CONTENTS .....	viii
LIST OF TABLES .....	x
LIST OF FIGURES .....	xi
LIST OF ABBREVIATIONS .....	xii
CHAPTERS	
1. INTRODUCTION .....	1
1.1. Background .....	1
1.2. Motivation.....	3
1.3. Contributions of the Study .....	4
1.4. Organizations of the Dissertation .....	6
2. BACKGROUND AND LITERATURE REVIEW .....	7
2.1. Geometric properties and non-linear growth model.....	7
2.2. Predicting the Aneurysm Growth using Probabilistic Programming .....	8
2.3. Cardiovascular Modelling for an Abdominal Aortic Aneurysms (AAA) .....	10
2.4. Summary of Background and Literature Review .....	11
3. MATERIALS AND METHODS .....	13
3.1. Study Design and Populations .....	13
3.2. Geometric Properties and Non-Linear Growth Model of AAA.....	15
3.2.1. Growth rates and their correlation analysis .....	16
3.2.2. Exponential AAA growth model and the growth prediction.....	17
3.3. Developing a probabilistic model for prediction of future AAA growth .....	18
3.3.1. Exponential AAA Growth Model .....	19
3.3.2. Patient-oriented Growth Prediction Model (POGPM).....	24
3.3.3. Generalized Linear Model (GLM) enhanced POGPM .....	25
4. RESULTS .....	27
4.1. Correlation Analyses and Defining master curve of AAA growth .....	27
4.1.1. Maximum measurements for correlation analysis .....	27
4.1.2. Growth rates and correlation analysis .....	28
4.1.3. Growth curve of the geometric measurements .....	29
4.2. Probabilistic Programming for Patient-Oriented AAA Growth.....	31
4.2.1. Posterior distribution of population (PDoP) .....	31
4.2.2. Patient-oriented prediction of AAA growth .....	33
4.2.3. Enhanced prediction of AAA growth.....	35

5. DISCUSSION.....	39
5.1. Defining master curve of AAA growth and its potential utility of clinical management .....	39
5.2. The prediction capability of the growth model .....	41
6. CONCLUSION .....	47
6.1. Limitation and Future Works .....	48
REFERENCES .....	51
APPENDICES .....	59
APPENDIX A.....	59
APPENDIX B.....	71
CURRICULUM VITAE .....	73

## LIST OF TABLES

Table 1. The information about longitudinal CT scan data .....	14
Table 2. The definitions of geometrical measurements .....	14
Table 3. Correlations of geometrical parameters on AAA actual measurements .....	28
Table 4. Correlations of geometrical parameter rates of change on AAA measurements using non-linear growth model.....	29
Table 5. The mean and standard deviation of each category, and their paired t-test results. ....	35
Table 6. The mean and standard deviation of each category, and their paired t-test results. ....	36
Table 7. The percentage of scans accurately modeled using PDoP, the POGPM and GLM enhanced POGPM .....	37
Table 8. The state of the art comparison .....	43

## LIST OF FIGURES

Figure 1. Anatomy of abdominal aortic aneurysm (AAA) .....	2
Figure 2. The representation of geometrical measurements derived from 3D constructed AAA .....	16
Figure 3. The iterative algorithm to find the master curve in Eq.3 .....	18
Figure 4. Predicting aortic aneurysm growth using patient-oriented growth models with two-step Bayesian inferences .....	19
Figure 5. The work-flow diagrams for POGPM (top) and GLM enhanced POGPM (bottom).....	24
Figure 6. Box and whisker plots for the growth rate of the diameters and aneurysm volume using non-linear model .....	28
Figure 7. The exponential functions of maximum spherical diameter (left) and maximum orthogonal diameter (right). .....	30
Figure 8. The prediction of AAA growth based on the master curve (spherical diameter).....	30
Figure 9. The frequencies of estimated parameters for the PDoP growth model and parameter values from drawn samples .....	31
Figure 10. The estimated parameters of the posterior distribution .....	32
Figure 11. The observed scans and aneurysm growth model based on the estimated parameters of PDoP. ....	33
Figure 12. An example of the demonstration for the prediction capability of a POGPM at 77th months and at 59th months.. .....	34

## **LIST OF ABBREVIATIONS**

<b>AAA</b>	Abdominal Aortic Aneurysm
<b>ANOVA</b>	Analysis of Variance
<b>CI</b>	Confidence Interval
<b>CTA</b>	Computed Tomography Angiography
<b>DIA</b>	Diameter
<b>ECC</b>	Eccentricity
<b>EVAR</b>	Endovascular Aortic Repair
<b>FEM</b>	Finite Element Method
<b>GLM</b>	Generalized Linear Model
<b>G&amp;R</b>	Growth and Remodeling
<b>HMC</b>	Hamiltonian Monte Carlo
<b>ILT</b>	Intraluminal Thrombus
<b>MAP</b>	Maximum A Posteriori
<b>MAX</b>	Maximum
<b>MCMC</b>	Markov Chain Monte Carlo
<b>MIN</b>	Minimum
<b>MRI</b>	Magnetic Resonance Imaging
<b>NUTS</b>	No-U-Turn Sampler
<b>PDF</b>	Probability Density Function
<b>PD<sub>o</sub>P</b>	Posterior Distribution of Population
<b>PER</b>	Perimeter
<b>POGPM</b>	Patient-Oriented Growth Prediction Model
<b>QoI</b>	Quantity of Interest
<b>TORT_CL</b>	Tortuosity of centerline
<b>VOL</b>	Volume

## CHAPTER 1

### INTRODUCTION

#### 1.1. Background

An abdominal aortic aneurysm (AAA) is a vascular disease diagnosed as a local permanent dilatation of the abdominal aorta, such that it is 50% larger than the normal vessel diameter (30 mm or more) [1], [2], and its volume gradually increases over years to decades. Each one of 1000 people between 60 and 65 years old has an AAA disease, which is more common among men and smokers [3], [4]. Although aneurysms are seen in different regions of the aorta, they usually occur in the abdomen and their growth during the disease without showing any symptoms in 7 out of 10 patients. Therefore, the diagnosis of the disease is usually rendered by other reasons for medical imaging such as ultrasound, CT or X-ray in abdomen or for physical examination coincidentally. The rupture of an AAA, having high mortality rate, is eventually observed if no surgical intervention (either open surgery repair or endovascular aortic repair - EVAR) is performed. This is a condition requiring an immediate intervention, and it is the 13<sup>th</sup> most fatal disease in the U.S [5]. Therefore, long-term monitoring is recommended prior to any surgical intervention for a small AAA. Figure 1 visualizes the anatomy of an abdominal aortic aneurysms.

The evaluation of the aneurysm development is not straightforward because it can only be assessed by monitoring the AAA without any intervention. In addition, the surgical intervention has its own risk and is therefore suggested principally based on the maximum diameter of the aneurysm (5.5 cm for men, 5.0 cm for women) or annual aneurysm growth (1 cm per year) [6], [7]. A rapid expansion of AAAs is often associated with higher rupture risk [8], and it has long been suggested that annual growth rate may play a critical role in prognosis, surgical planning, and patient management. However, 10–24% of aneurysms below the intervention threshold (< 55mm) experience rupture as shown in some series [9], [10]. Unnecessary surgery is another problem encountered today, having its own risk and high cost. 473 non-repaired AAAs examined from autopsy reports indicate that 60% of the AAAs greater than 5 cm (including 54% of those AAAs between 7.1 and 10 cm) do not experience

rupture [11]. Furthermore, the rupture might also occur when the annual growth rate is less than 1 cm. Limet et al. [12] reported that the rupture risk was 10% if the annual growth rate is between 0.2-0.5 cm and the initial aneurysm diameter size is between 4.0 and 5.0 cm. Therefore, the guideline for the non-surgical management of AAA reported that one of the unresolved issue was the development of better predictive tools for individual rupture risk including morphology based indicators.

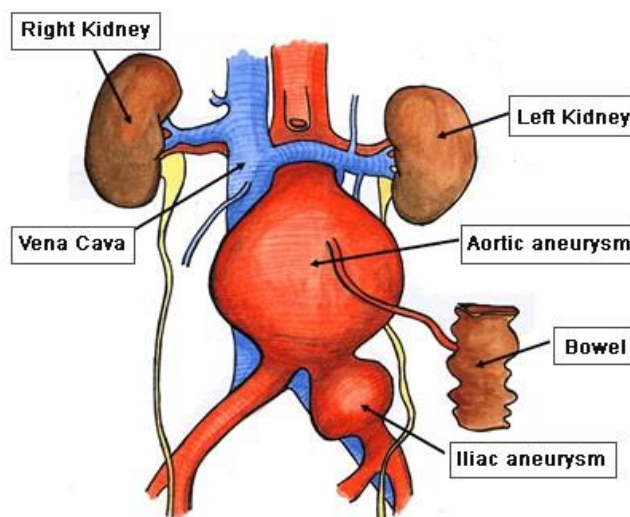


Figure 1. Anatomy of abdominal aortic aneurysm (AAA)

There are various measurements demonstrated in previous studies to describe aneurysm evaluation over the time. A regular ultrasound screening for aneurysms smaller than 5.5 cm is recommended in international guidelines to prevent mortality due to ruptured AAA. For example, an annual ultrasound scan is recommended for aneurysms between 3 and 3.5 cm while biannual scan is recommended for AAAs between 4.5 and 5.5 cm in diameter as previous work demonstrated that future AAA growth strongly depends on the initial diameter [13]. However, there is no standard protocol to measure the maximum diameter of an AAA since the shapes of these aneurysms are highly varied and irregular. The maximum diameters of an AAA estimated on the axial and orthogonal planes perpendicular to the aorta centerline are commonly used for medical decision, and the previous studies have reported their investigation for their prediction capability and reproducibility [14], [15]. The aneurysm volume, an alternative measure to maximum diameters, was proposed by several studies to assess the development of AAA and to evaluate the rupture risk potential [14]–[16]. The volume measurement is, however, not practical in the clinical setting. Meanwhile, the morphology of aneurysms was found to play an important role, affecting the rate of growth and risk of rupture. For example, previous studies reported that some parameters such as asymmetry and tortuosity [17], and ratio of ILT to AAA volume [18] were associated with risk of rupture. Similarly, the geometrical changes in terms of the surrounding tissues [19], the patients' age and gender were also used to describe aneurysm evolution over time. To sum up, there is no common



consensus reached out on which measurements are the best representative of the aneurysms' state and mathematical models of their future growth patterns (e.g., linear or exponential growth) are.

The variability of AAA expansion rates is still high among patients [20], but why some patients have AAAs with accelerated expansion rate, and why others with identical risk profiles do not remain unclear [21]. This makes predicting the natural growth pattern difficult because the aneurysm growth over the time does not necessarily follow the common pattern for all patients [16][17]. Thus, developing a reliable tool having the capability of predicting future AAA growth rate is important in terms of surgical planning and patient management. A recent study [23] based on 227 responses from vascular/endovascular surgery colleagues showed that “discovering new tests to predict an AAA will be fast growing” and thus should be one of the top priorities for research. Furthermore, successful tools helpful for per-patient basis treatment planning were demonstrated by previous studies [18][19]. For example, Lee et al. demonstrated the strength of the prediction capability of a patient-oriented growth with a biomarker of flow mediated dilation exploiting machine learning techniques [26]. Liangliang et al. developed an appealing computational framework and incorporated with patient-oriented anatomical information to accurately predict individual shapes of AAAs associated with an uncertainty [27].

The next is followed by various analytic approaches for AAA growth prediction. First, we categorized those literatures to biological tissue growth and remodeling (G&R, biomechanical modeling), supervised machine learning and probabilistic forecasting modeling (our study) which explained the techniques relevant to. Second, we compared the limitations of these analytic approaches. Finally, we explained why our approach would be feasible; and we compared with other provided solutions by giving the strengths of our approach as well as by considering the main limitation of approaches previously mentioned.

## **1.2. Motivation**

Surgical repair is vital for the patient before rupture. The maximum diameter measurement of abdominal aortic aneurysm (AAA) plays significant roles in the clinical decision making process. However, the diameter measurements depend on the way of extracting orthogonal and axial cross-sections or maximally inscribed spheres within the AAA surface. The guideline for clinical AAA management based on the single maximum diameter criterion has been challenged [12], [28]–[30] with more studies proposing that the growth rate is associated with AAA rupture [30], [31]. There is, however, scarcity of morphological studies using longitudinal CT scan images. Therefore, the main aim of this study is to construct a larger database of morphological parameters and to enhance the predictability of AAA growth for high-risk aneurysms.

In this study, we constructed anatomic 3D models of the AAAs in 118 longitudinal Computed Tomography (CT) scans from 26 Korean AAA patients. We subsequently

analyzed 21 derived geometrical measurements for each, their growth rates, and their pairwise correlations, and attempted to enhance the predictability of the growth for high-risk aneurysms. Furthermore, 3D volume rendering of an AAA with different scale of colors appropriate for hemodynamic forces were provided to clinicians, so they might have opinion about the aneurysm structure and specifically regions having high rupture risk prior to a surgical operation.

In this way, we tried to find answers for the following research questions.

- What are the correlations between the morphological parameters and which one is the best representative of the aneurysm growth?
- Is it possible to discover a new probabilistic model which determines if an AAA will be fast growing and to develop a tool that has the capability of predicting future AAA growth based on time?
- How the process of surgical planning and patient management is clinically improved during the surveillance?

Basically, this study tested a hypothesis of if a growth pattern of AAAs exists in a patient group. While other previous studies emphasized the difficulty of predicting aneurysm expansion, we used various geometrical measurements and selected the one that gives the least of variation, which fits to one curve, called the master curve. To do so, we used an iterative fitting method by shifting individual growth curves along the time axis by minimizing the total errors. Once the population-based curve (called a master curve) is defined, the next diameter is predicted by using the parameters of the master curve and follow-up time along the shared time axis. Thus, the diameter at the time of the next scan could be predicted. Furthermore, using a two-step approach based on Bayesian calibration, a significant progress has been made toward patient-specific AAA growth modeling in this study. An exponential growth model was built specifically on patient characteristics using geometrical measurements.

### **1.3. Contributions of the Study**

A total of 21 measurements of the aneurysm's 3D geometry, reflecting the properties of the aneurysm at the time of the scan, were classified as either primary or secondary and analyzed in terms of their correlations for each observation. In addition, the growth rate for each measurement was calculated in a non-linear fashion, and their pairwise correlations were also analyzed. One of the findings from the correlation analysis on the morphological parameters is that the total volume is highly correlated with all primary parameters (maximum diameters, perimeter) which increases by the expansion of overall AAA volume size. Meanwhile, there has been increasing evidence that the growth rate is important for predicting high rupture risk. Compared to the correlation between diameter measurements, AAA volume expansion rates are only mildly correlated with the spherical and orthogonal growth rates.

We examined the utility of master curves and their prediction capabilities in terms of different geometrical parameters. Among all the parameters, the master curve of spherical diameter performed best, predicting the diameter within 0.42 mm in 95% of all scans. In addition, we observed that the master curve using the spherical diameter resulted in a small prediction error, while those of orthogonal and axial diameter have resulted in larger errors. Therefore, we proposed that a master curve for spherical diameter may be used as a clinical tool that gives insight about the future of the aneurysm growth, and facilitates planning of follow-up scans and surgical interventions.

We further validated the applicability of this work and regressive power of both the model and the regressor using data from a Korean AAA cohort. The spherical diameter was found as the best representative of the growth curve since it has the least fluctuations and narrowest range in measurements. Thus, the growth curve, named the master curve, was obtained to summarize the growth with a significantly higher prediction strength compared to other measurements and to evaluate the prediction accuracy for each measurement.

How the proposed model enhances the prediction of AAA growth rate can be summarized as follows:

- An exponential growth function was adapted rather than the traditional linear model,
- 21 geometric measurements were systematically examined to enhance the prediction capability of the growth rate, and it was found that the spherical diameter was the single most predictive feature based on the exponential model.

This study also developed an enhanced prediction growth model applicable for predicting AAA growth accurately using Bayesian inference. An exponential growth model, commonly demonstrated in the previous studies, is selected, and the estimated parameters of the posterior distributions which were adopted from given observations (scans). This study used 106 CT scans from 25 patient dataset to construct Posterior Distribution of Population (PDoP) and further predicts patient-specific AAA growth.

PDoP based Bayesian inference method with an exponential function showed that 79% of all scans within 2.67 mm error can be predicted using PDoP with 0.95 confidence interval. There are, however, 21% of all scans which were not followed the common properties of the population. The percentage of observed scans that the diameter growth was over- and under-estimated were 5 (n=4) and 16 (n=13) respectively. On the other hand, these number are 5 (n=4) were 12 (n=10) in Patient-Oriented Growth Prediction Model (POGPM). The 23 % of previously overestimated scans (n=13), were accurately modeled within tolerance, if the POGPM, specified according to an individual characteristic, was used. Generalized Linear Model (GLM) enhanced POGPM were also used to take the tortuosity of centerline into account in the growth model and decrease the chance of inaccurate prediction due to cases of

sudden growth. The percentage of observed scans that the diameter growth was over- and under-estimated were 5 (n=4) and 9 (n=7) respectively in GLM enhanced POGPM.

The prediction model was built specifically on patient characteristics using the various geometrical measurements. This enhanced the prediction capability of a measurement at any time-point, along with an evaluation of the associated with uncertainty. The proposed tool might be helpful clinically, especially for a rapid expansion of AAA, often associated with higher rupture risk, in terms of elective surgical intervention and patient management.

Although the main motivation behind the study is finding a model which helps clinicians to effectively manage the prognosis of AAA patients, we have also contributed to how a 3D model of an AAA sac can be constructed, and hemodynamic forces using a number of open source software can be measured, which is in the APPENDIX.

#### **1.4. Organizations of the Dissertation**

The dissertation consists of six main chapters, namely Introduction, Background and Literature Review, Materials and Methods, Results, and Discussion and Conclusions. All the details of the geometrical evolution of AAA during surveillance and the proposed prediction framework within the context of this study are given in the following chapters.

## **CHAPTER 2**

### **BACKGROUND AND LITERATURE REVIEW**

This chapter briefly discusses the background and literature related to this study. The literature review is laid out in three main sections: (1) geometric representation of an AAA, correlation analyses and non-linear growth model; (2) developing probabilistic models for prediction of future AAA growth; and (3) creating solid models of AAA and blood flow simulations. The chapter is concluded with summary of background and literature review section.

#### **2.1. Geometric properties and non-linear growth model**

An abdominal aortic aneurysm (AAA) is characterized by a permanent dilation of the abdominal aorta (30 mm or more) [1], [2]. The decision to intervene is made based on AAA size measured by a maximum diameter (5.5 cm for men, 5.0 cm for women) or its growth rate (1 cm per year) [6], [7]. For small AAAs, long-term monitoring is recommended prior to any surgical intervention (open surgery or endovascular aortic repair (EVAR)). However, 10 – 24% of aneurysms below the intervention threshold (< 55mm) experience rupture as shown in some series [9], [10]. Therefore, the guideline for the non-surgical management of AAA reported that one of the unresolved issue was the development of better predictive tools for individual rupture risk including morphology based indicators. Additionally, a rapid expansion of AAAs is often associated with higher rupture risk [18], [32], [33], and it has long been suggested that the annual growth rate may play a role in prognosis, surgical planning, and patient management.

Although time-dependent geometrical analysis is a significant part of the clinical decision making process, quantification of the expansion rate remains ambiguous. Multiple studies have suggested that variability of AAA expansion rates is high, both over time in the same patient and among various patients [34], [35]. Furthermore, finding the natural growth pattern is difficult as the change of diameter is small and non-linear [36]. Studies have also reported that growth rates are not constant; instead, periods of active rapid growth are followed by periods of non-activity [37], [38]. However, others have suggested a general AAA growth pattern in which an AAA

expands over time with an increasing expansion rate as it gets larger [2], [33], [39]–[41].

There are uncertainties about AAA measurements and evaluating AAA expansion rate is not clinically routine [42]–[44]. Two common approaches measuring diameter are documented in previous studies [28], [43], [45]: the maximum diameter on axial plane (“axial diameter”) and orthogonal plane perpendicular (“orthogonal diameter”) to the aorta centerline. These studies claimed that orthogonal diameters represent the size of AAAs better, while axial diameter is more robust in terms of reproducibility of the measurements. Gharahi et al. [39], hence, suggested a method (“maximally inscribed spherical diameters”) based on the maximum spheres inscribed throughout the AAA that generated the centerline. With a longitudinal CT data set obtained from 14 patients, they showed that the spherical diameter measurement gives the least variability, compared to axial and orthogonal diameter measurements. In addition, they proposed that an exponential function fits the AAA growth pattern. These preliminary results call for a more extensive study on the AAA morphological growth patterns and the correlation between geometrical characteristics and their growth rates. Furthermore, this study investigates whether there exists a potential population-based pattern of AAA growth rate for a specific group of patients. This work will explore the idea of a “master curve” for AAA growth, and the parameters which best enhance its predictability for clinical use.

In a summary, there is no consensus on what the general AAA growth pattern is, nor what the universal AAA measurement should be. Furthermore, the best geometric parameter for predicting aneurysm growth is still under question. Hence, this study used a series of longitudinal CT scan images retrospectively obtained from Korean patients and geometrical measurements that represent the AAA and estimate its growth rates were derived. The objective of this study is to investigate correlation of these measurements and find the best parameter describing the growth as a potential representation of the AAA using longitudinal CT data.

## **2.2. Predicting the Aneurysm Growth using Probabilistic Programming**

The evaluation of the rupture risk is not easy because it's true risk can only be assessed by a follow-up monitoring of the AAA without any surgical intervention. On the other hand, the surgical interventions have their own risk and such an intervention is therefore recommended only when the maximum diameter of the aneurysm reaches to 55 mm or annual aneurysm growth exceeds to 1 cm per year [12]. Thus, developing a tool, having a capability of prediction of future AAA growth rate which is revealed by subsequent measurements, is important in terms of the surgical planning and patient management. A recent study received the 227 responses from vascular/endovascular surgery colleagues and showed that “discovering new tests to predict an AAA will be fast growing” is the top priorities for research accordingly [27].

There have been several papers [12], [28]–[30], wherein the traditional guideline for clinical AAA management based on a single criterion has been challenged; alternatives have been proposed which take into account various factors such as growth rate [3][6], AAA volume [28], thrombus accumulation [46], asymmetry and tortuosity [8][9] for improved assessment of aneurysm development and rupture risk. Particularly, there is a recent consensus that the growth rate is critical for AAA clinical management even for small diameter AAAs [49].

We analyzed the derived 21 geometrical measurements, because there is no common consensus reached on which of the measurements is the best representative of the aneurysms evaluation and what is a general AAA growth pattern. We found that the spherical diameter might be the best representative of the growth curve (r-square: 0.985) using non-linear model, which might be used to predict AAA growth (74 of 79 scans were accurately predicted within 2.1 mm error). However, there were two major limitations presented in the study: an analytic solution, which is not feasible for the most non-trivial models for calculating the posterior estimates, is used and a point estimate without any confidence was provided even though the reported precision of scan measurements is usually  $\pm 2$ mm. Furthermore, the lower accuracy for the patients having relatively faster or slower AAA growth was observed, because the model was mainly established for reflecting the population common characteristics. In this study, the major limitations represented in our previous study were bounded by up-to current advancement of probabilistic programming.

Motivated by recent studies, this study aims to develop a tool that detects patients who have fast growing AAAs and predicts the growth rates of their respective aneurysms during surveillance. There has been substantial heterogeneity of AAA growth rates among various studies; some studies reported that 11.4% [12] and 12% [50] of AAAs stop expanding, while others reported that AAA diameter size was associated with increases of growth rate [8]. The difficulty of AAA growth rate prediction was exacerbated by the high uncertainty of different diameter measurements so Gharahi et al. [29] suggested an alternative, semi-automatic method of measuring the maximally inscribed spherical diameter, reducing uncertainty in measurements. Akkoyun et al. [51] then investigated the correlations among 21 geometrical measurements of retrospectively obtained longitudinal CT scan images and concluded that “spherical diameter” could be the most accurate predictor representative of the growth curve.

Significant progress has been made toward patient-specific AAA growth modeling to assess the rupture risk using biological tissue growth and remodeling (G&R) and machine learning [18][19]. Zeinali-Davarani et al. presented patient-specific modeling of an AAA, which is able to trace alterations of the geometry [25]. G&R models used finite element method (FEM) to simulate the exact mechanical state of an AAA at a given time but do not accommodate the uncertainty in their predictions [52]. There is emerging evidence that the geometrical properties of an AAA might provide more valuable information for predicting AAA growth [26]. Shum et al. [53] derived 28 geometrical measurements from 76 CTA scans describing the size and shape of the

aneurysm, and developed a model capable of discriminating aneurysms as ruptured and unruptured with an accuracy of 86.6%. Similarly, Parikh et al. [54] investigated geometrical indices derived from 75 electively and 75 emergently repaired AAA scans, and revealed the three most significant indices in the classification of an AAA (with an average accuracy of 81.0%) using decision trees, a machine learning algorithm. Similarly, Lee et al. [26] applied a non-linear support vector regression (SVR) model to predicting patient-oriented growth with an additional biomarker, flow mediated dilation.

Probabilistic programming techniques are gaining mainstream interest in biomedical research. In this study, a two-system approach based on Bayesian calibration [24] was used and the aneurysm growth model was specified according to individual patient characteristics. The distribution estimates based on a summarization of samples drawn from the specified model using Markov Chain Monte Carlo (MCMC) samplers [20]. This estimation is made practical by using automatic Bayesian inference on a user-defined probabilistic model, which fundamentally enhances our subjective belief by the probability of an event via incorporation of experimental data [26,27]. Although the idea of using a MCMC for Bayesian inference is not novel [27], [28], [29], it has not been reported in the AAA's diameter estimation before. The unique computational advantages of this powerful approach, incorporating prior belief and observed scans, prediction of diameter associated with uncertainty at any time-point, capability of taking into a patient individual characteristics and other geometry account, were all yielded to assessment of the aneurysm growth.

To this end, an exponential growth model was built specifically on patient characteristics using 21 geometrical measurements derived from 106 Computed Tomography (CT) scan images. Thus, the prediction of a measurement at any time-point can be made, along with an associated uncertainty to provide a clinically helpful tool for surgical planning and patient management during the surveillance of abdominal aortic aneurysms.

### **2.3. Cardiovascular Modelling for an Abdominal Aortic Aneurysms (AAA)**

Most small aneurysms have no symptom and were considered safe, while large aneurysms may be fatal in the case of rupture, which causes massive internal bleeding. Aneurysm repair prior to rupture is thus vital. Scientific research has shown that the criterion is not accurate for predicting aneurysm risk (Vorp et al, 2007; Limet et al. 1991) and it is necessary to consider other parameters for assessing risk. Furthermore, visualizing the 3D model with a color map is very useful to surgeons before the operation. In this study, biomechanical behavior of the aneurysm is analyzed within the context of hemodynamic forces such as wall shear stress and velocity pattern in order to better understand the reasons for gradual aneurysm growth and potential rupture.



The morphology of an AAA is more complex than an idealized vessel or a healthy aorta. Enhancement and segmentation of an aorta within the computed tomography image also required additional attention and applying specialized techniques. Using just SimVascular platform might not be sufficient to obtain simulation results, although applying the same procedure given in the user guide is enough for an idealized vessel structure. Obtaining a solid model from a CT image is another issue, since using 2D segmentation on a number of the preferred slices rather than all ones might lead to loss of the critical information. Furthermore, an automatic segmentation of an AAA from the surrounding tissue, especially for vein, is not always applicable.

ITK-Snap is an open source software was used for segmenting the lumen in 3D based on the active contour algorithm. The tool has an ability to visualize the progress online on anatomical planes. SimVascular can use Navier Stokes equation for the biomechanical modelling of an aorta aneurysm but it requires complete mesh of the model. Therefore, constructed 3D model were migrated into SimVascular platform, where the faces and meshes can be defined properly. Then, we run the analyses for a period of time and get the results in a single file with a vtu extension. It is not possible for SimVascular to visualize its result, an open source software (ParaView), therefore, was used for this purpose.

Although a patient-specific blood flow simulation and analyses is out of the scope of the thesis study, we presented an end-to-end procedure that can be used to construct 3D models of the aneurysm and run hemodynamics simulations with realistic choices for flow parameters and profiles. The steps required for modeling the biomechanical behavior of an AAA with its proper software were summarized as following, and a useful guideline having detail about each step was given in APPENDIX.

- Gdcm2vtk library on Linux OS
  - Translating DICOM image series into VTK file format
- ITK-Snap
  - 3D segmentation using an active contour algorithm
  - Solid model construction in VTP file format
- SimVascular
  - Mesh generation
  - Face identification
  - Preparing input file for simulation
  - Defining boundary conditions
  - Running numerical simulation
- ParaView
  - Visualization aneurysm with color map

## **2.4. Summary of Background and Literature Review**

In this section, background information and an overview over the relevant literature are presented. The evolution of the aneurysm development is critical and not

straightforward because it can only be assessed by monitoring the AAA without any intervention. Therefore, various measurements demonstrated in previous studies to describe aneurysm evaluation over the time. There is, however, no common consensus reached on which measurements are the best representative of the aneurysms' state, and their future growth patterns such as linear or exponential growth. In this study, we used 3D models of the AAAs in 118 longitudinal Computed Tomography (CT) scans, from 26 Korean AAA patients. We subsequently analyzed 21 derived geometrical measurements for each, their growth rates, and their pairwise correlations, and attempted to enhance the predictability of the growth for high-risk aneurysms. On the other hand, probabilistic programming techniques are gaining mainstream interest in biomedical research. In this study, a two-system approach based on Bayesian calibration [24] was also used, and the prediction of a measurement at any time-point can be made, along with an associated uncertainty. Although, the main motivation behind the study is finding a prediction model, which helps clinicians to effectively manage the prognosis of AAA patients during the surveillance, we have also prepared a guideline about how to construct a 3D model of an AAA and calculate hemodynamic forces using open source software and tools, which are free and flexible to make research. A useful guideline was given in APPENDIX.

## **CHAPTER 3**

### **MATERIALS AND METHODS**

This chapter consists of four subsections. Each subsection uses a different methodology, and details are presented in this chapter. Firstly, 21 different parameters describing the geometric properties of each CT scan were used and their growth rates as well as pairwise correlations were analyzed. Afterwards, the best representatives of the master curve, constructed for the measurements to predict aneurysm growth, were selected based on their r-square scores. As a parallel study, a two-system approach based on Bayesian calibration was used and the aneurysm growth model was specified according to individual patient characteristics. Thus, the prediction of a measurement at any time-point can be made, along with an evaluation of the associated uncertainty.

#### **3.1. Study Design and Populations**

The retrospective data set used in this study is geometrical measurements describing the properties of AAA morphology. 118 computed tomography (CT) scans from 26 patients obtained retrospectively at the Seoul National University Hospital were used for this analysis. Patients were followed and scanned at various time intervals between 3 to 56 months with a median interval of 11 months. Images were obtained using a CT scanner (Siemens Healthcare, Erlangen, Germany). Image in plane resolution was 0.641 mm and in a transverse (z-axis) resolution of 1 mm. This study was subject to Internal Review Board approvals at Michigan State University and Seoul National University Hospital. Since our study does not involve identifiable human subjects, and only processes anonymized and archived CT scans, the need for ethical approval was waived by the Michigan State University Institutional Review Board (reference: IRB# 12-1041).

All AAAs with at least two CT scans and a time interval of at least 6 months were used for this study. This inclusion criterion was made in order to minimize the growth rate error. As a result, 106 CT scans from 25 patients (23 men and 2 women) were used and 21 different parameters describing the geometric properties of each scan were calculated. The mean age at time of first scan was 59 years old (55-84), with a 13-month mean time between scans (6-56), and 4 scans per person (2-7). Table 1 shows the demographic information of patients.

Table 1. The information about longitudinal CT scan data

Age (year)	69 (55-84)*
Men (n)	23
Women (n)	2
Interval between consecutive scans (months)	13 (6-56)
Scans per patient (n)	4 (2-7)

\*The age at which the first scan was taken is given by mean and range

From these CT images, AAA geometries were reconstructed using Mimics (Materialise, Leuven, Belgium), following the procedure previously described (Gharahi et al. [39]; Kwon et al. [55]) and used to generate centerlines with the *maximally inscribed spheres* method. A series of slices perpendicular to the centerline (orthogonal planes), or to the Z-axis (axial planes), were made with a constant interval distance, such that the intersection of these planes with the AAA surface produced the cross-section required to measure the orthogonal or axial parameters.

The definitions of all geometrical measurements, which were classified as either primary or secondary parameters, are summarized in Table 2. These parameters reflect the local and global properties of the aneurysm at the time of the scan and details of maximum diameter measurements are described by Gharahi et al [39].

Table 2. The definitions of geometrical measurements

	Parameter	Description
<b>Primary</b>	MAX <sub>DIA_S</sub>	the maximum inscribed spherical diameter in mm
	MAX <sub>DIA_A</sub> , MAX <sub>DIA_O</sub>	the maximum axial and orthogonal diameter in mm
	MAX <sub>PER_A</sub> , MAX <sub>PER_O</sub>	the maximum perimeter on axial and orthogonal planes in mm
	DIA <sub>PER_A</sub> , DIA <sub>PER_O</sub>	the perimeter on axial and orthogonal planes at the maximum spherical diameter in mm
	VOL <sub>AAA</sub>	the total volume of the aneurysm in mm <sup>3</sup>
<b>Secondary</b>	VOL <sub>ILT</sub>	the total volume of the thrombus in mm <sup>3</sup>
	VOL <sub>LUMEN</sub>	the total volume of the lumen in mm <sup>3</sup>
	MIN <sub>DIA_A</sub> , MIN <sub>DIA_O</sub>	the minimum diameter on axial and orthogonal planes in mm
	MAX <sub>ECC_A</sub> , MAX <sub>ECC_O</sub>	the maximum eccentricity on axial and orthogonal planes
	DIA <sub>ECC_A</sub> , DIA <sub>ECC_O</sub>	the eccentricity on axial and orthogonal planes at the maximum spherical diameter
	MAX <sub>ILT</sub>	the maximum thrombus thickness in mm
	A <sub>ILT</sub>	the fraction of AAA surface area covered by ILT content
	MDIA <sub>TORT_DISP_A</sub> , MDIA <sub>TORT_DISP_O</sub>	the displacement of the AAA centerline from the line joining the first and last points of the AAA centerline at the maximum diameter cross section, on axial and orthogonal planes
	TORT_CL	the ratio of the total centerline length to the length of the line joining the first and last point

Eccentricity was defined as the ratio of maximum to minimum diameter and was calculated for both orthogonal and axial planes. Tortuosity of the centerline was calculated as the ratio of the total centerline length to the length of the line joining the first and last point. Finally, perimeter is found by measuring the length of the line forming the boundary of the aneurysm shape in the cross-sectional plane.

Volume measurements, denoted as VOL, include lumen volume, total AAA volume, and calculated intraluminal thrombus (ILT) volume (subtracting the total lumen volume from the total AAA volume). The global maximum and minimum of a local measurement in AAA geometry were denoted by MAX and MIN, respectively.

Patients were monitored and scanned at various time intervals between 6 to 56 months with a median interval of 11 months. 81 of the 106 scans were used for diameter prediction, as the first scan of each patient (i.e. the baseline) is assumed to be known, and required, for the prediction of subsequent diameters. Therefore, one scan per patient (for a total of 25 scans) was excluded from the follow-up set, leaving 81. In addition to predicting the follow-up diameter at any arbitrary time, we also categorized the scans to time intervals of 6-18 and 18-30 months as 1st and 2nd year, respectively, to be able to compare the performance of the prediction models with other studies presented in literature, which use yearly time categories. Retrospective growth data were recorded at the 1st year ( $10 \pm 4$  months) in 68 scans and at the 2nd year ( $20 \pm 3$  months) in 8 scans. We did not categorize the remaining 5 scans, recorded after 30 months ( $44 \pm 13$  months).

### **3.2. Geometric Properties and Non-Linear Growth Model of AAA**

Within the scope of the thesis, the definitions of 21 different geometrical measurements, which were classified as either primary or secondary parameters, are summarized and their growth rates of each AAA patient at a given time was computed by considering changes in parameters between two consecutive scans. Figure 2 demonstrates the morphological parameters of an aneurysm sac. Finally, these measurements were analyzed to evaluate potential capability of growth prediction.

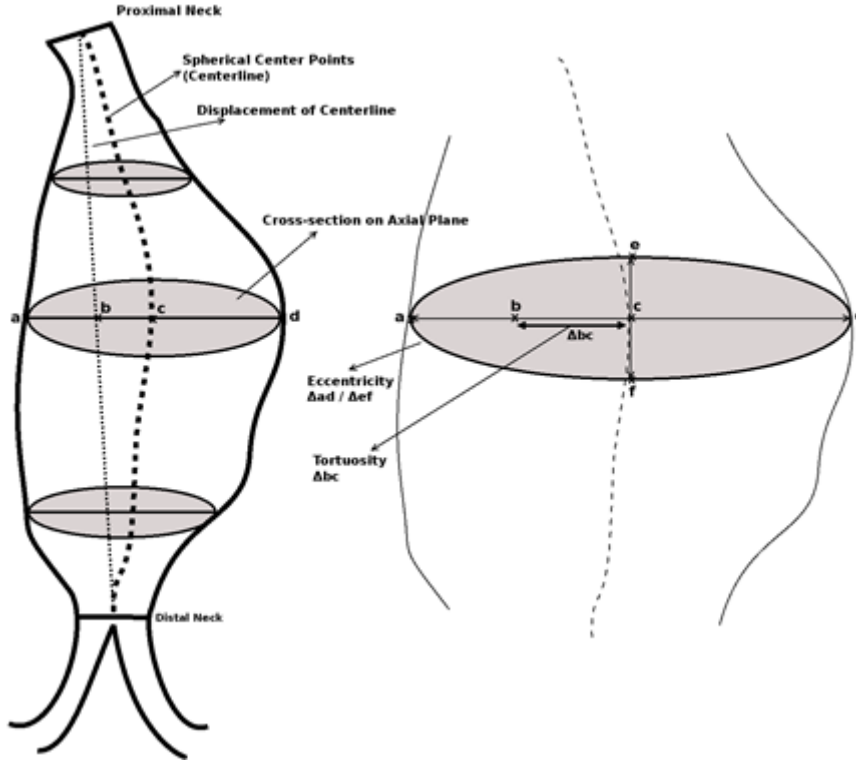


Figure 2. The representation of geometrical measurements derived from 3D constructed AAA

### 3.2.1. Growth rates and their correlation analysis

The growth rate of each AAA at a given time was computed by considering changes in parameters between two consecutive scans. The rate values for all measurements were calculated based on the assumption that there is an exponential change of the measurement over time. The rate of a parameter  $g(\cdot)$ , introduced in [40], is computed for all geometrical measurements by using the following equations

$$g = (e^{12r} - 1) \times 100 \quad (1)$$

where  $r$  is the logarithmic growth factor measured by

$$r = \frac{1}{t} \ln \frac{X_{followup}}{X_{baseline}}, \quad (2)$$

$X(\cdot)$  denotes the quantity of the geometrical measurements and  $t$  is the time interval between consecutive scans in months. For example,  $gMAX_{DIA\_S}$  was used to define the growth rate of maximum spherical diameter, where the maximum spherical diameters can be compared at baseline and follow-up. Pearson correlation coefficients were used for correlation analysis of different growth rates. We consider correlation ranges of 1.00–0.90, 0.90–0.75, 0.75–0.50, 0.50–0.25, 0.25–0.0 as very high, high, moderate, weak, and no correlation, respectively.

### 3.2.2. Exponential AAA growth model and the growth prediction

All geometric measurements were analyzed to evaluate potential capability of growth prediction. As proposed by Martufi et al. [40] the growth rate was expressed using an exponential function over the time. The growth curve is defined as an exponential function

$$Y = \alpha \times e^{\beta t}, \quad (3)$$

where  $Y$  is the measurement and  $\alpha$  and  $\beta$  are parameters of the growth curve. The input time  $t$  is the shared time axis for all the patients. Since the AAA stage of the patients at the time of first scan was not the same, the time of the scan must be shifted in the shared time axis. Exponential AAA growth model is based on the assumption that the individual growth patterns, the parameters of each growth curve ( $\alpha$  and  $\beta$ ) are identical to the master curve pattern. For this purpose, an initial growth curve is fitted ( $\alpha$  and  $\beta$ ) to one patient. Subsequently, the time of the first scan  $t_1^i$  is estimated using the method of least squares so that the measurement set best fits the common growth curve, where superscript  $i$  denotes patient data sets. These two steps are repeated, updating  $t_1^i$  at each iteration until convergence (i.e. total amount of error met the convergence criterion or no longer decreases) is achieved. Finally, the growth curve, named the *master curve*, was obtained using `fminsearch`, a built-in function of MATLAB software to find a local minimum for unconstrained nonlinear optimization based on the Nelder-Mead simplex algorithm. The pseudo-code of the algorithm was given in Figure 3.

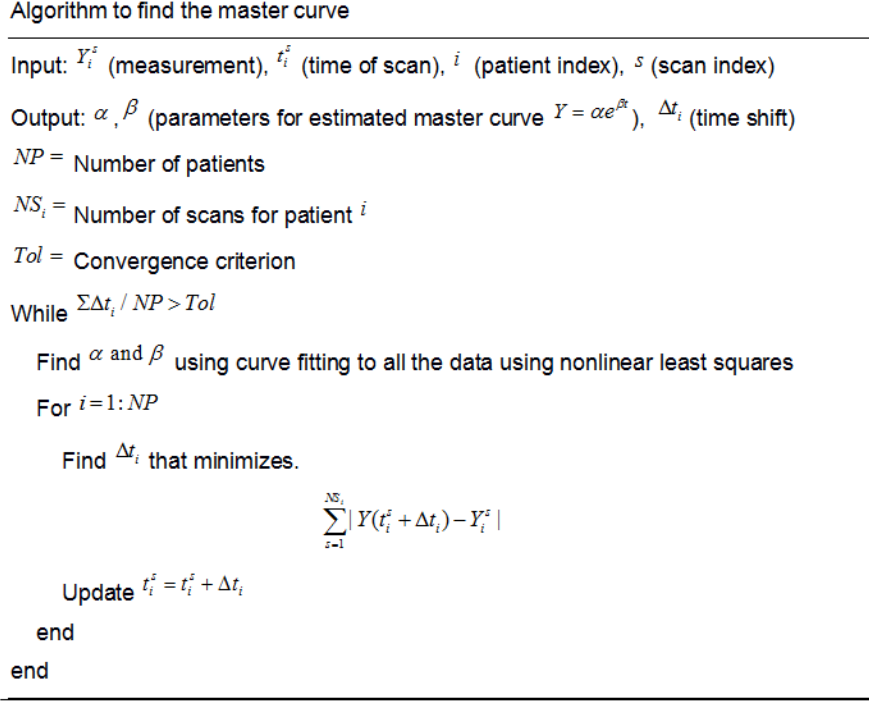


Figure 3. The iterative algorithm to find the master curve in Equation 3

The least fluctuations and narrowest range in measurements contributes to the prediction strength of the master curve, obtained to better summarize the growth and to evaluate the prediction accuracy for each measurement. The coefficient of determination, denoted by r-square, was utilized to measure how well growth was predicted [56], such that the minimum proportion of the total variance of outcomes explained by the model was selected as the most representative of the growth curve. The curve was log transformed from non-linear to linear and evaluated by r-square.

### 3.3. Developing a probabilistic model for prediction of future AAA growth

This study developed an enhanced prediction growth model applicable for predicting AAA growth using Bayesian inference. An exponential growth model, commonly demonstrated in the previous studies, is selected and the estimated parameters of the posterior distributions, the common properties of the population (our subjective belief), was fed to the prior for each patient's specific model. In addition to diameter, the study was extended using the Generalized Linear Model (GLM) to take other geometry properties into account. Thus, 106 CT scans from 25 patient dataset were used and the prediction of a measurement at any time-point can be made, along with an evaluation of the associated uncertainty. Figure 4 demonstrates the workflow of the study.



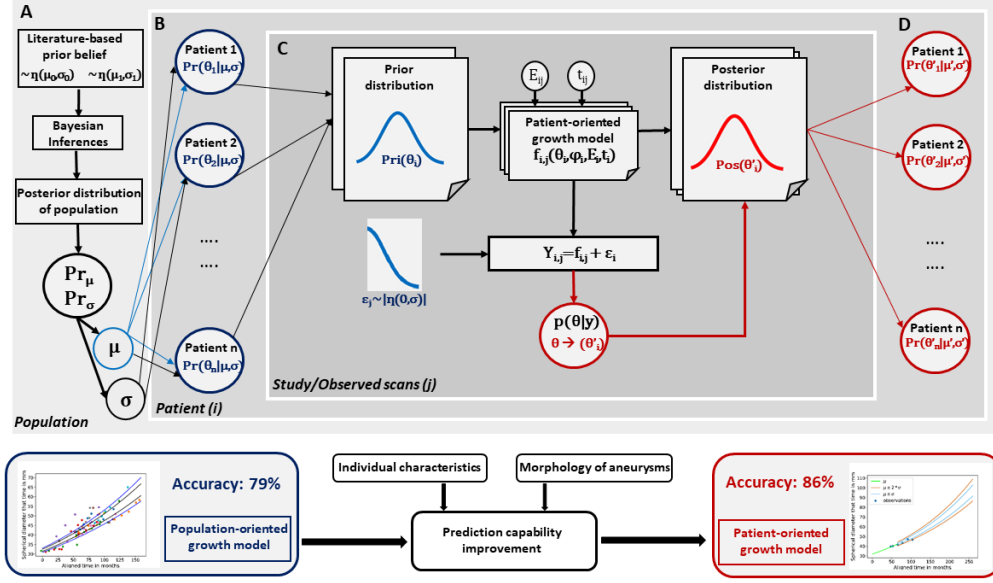


Figure 4. Predicting aortic aneurysm growth using patient-oriented growth models with two-step Bayesian inferences

In this study, a two-step approach based on Bayesian calibration was used and the aneurysm growth model was specified according to individual patient characteristics. At the first stage, the parameters of posterior distribution of population (PDoP) were estimated using the spherical diameter based on the whole population. Although we use a single feature to make a prediction, it is in effect still a conditional probability because it takes into account all previous measurements. At the second stage, the patient oriented growth prediction model (POGPM) is specified according to each patient individually, since each patient has different characteristics and growth rate.

### 3.3.1. Exponential AAA Growth Model

Previous studies demonstrated that the aneurysm growth should be modeled in a non-linear fashion [4,15]. In this study, we consider AAA growth model of the maximum spherical diameter, in which the diameter  $D$  at time  $t$  is given by

$$D(t) = \alpha e^{\beta t} \quad (4)$$

where  $\alpha$  denotes the initial maximum diameter at  $t=0$  and  $\beta$  denotes the diameter growth rate. In the analytic solution approach,  $\alpha$  and  $\beta$  are the parameters, each of which takes a constant value for a given data set.

## Bayesian Framework of Model Calibrations

A Bayesian inference technique employs to calibrate the growth model with clinical data and further predicts a future AAA growth of each patient. To test the prediction capability of AAA growth, a Quantity of Interest (QoI) is defined as the maximum spherical diameter expansion rate for per-patient and specific case. That is, each time point that a CT scan obtained was sequentially selected as a QoI, which enables us to determine a statistical model and investigate the associated uncertainties.

The scans were categorized into three classes: ‘over-estimated’, ‘under-estimated’ and ‘within tolerance’, based on whether the actual follow-up diameter was below, above, or within the 95% Confidence Interval (CI) of the estimate, respectively. We aimed to increase the number of scans that belong to ‘within tolerance’, which determines the performance of the prediction model.

Each individual patient has a varying number of sequential measurements over differing time lengths. These sequence of measurements were partitioned into two subsets; a calibration (DC, i.e. training) and a validation (DV, i.e. test) data set, as proposed by Hawkins-Daarud et al. [57]. The calibration set was used to calibrate the model, whereas the validation set was used for validation of the calibrated model. Apart from the initial scans, all scans in the population were incrementally and sequentially employed in validation to demonstrate whether our model predictions were consistent with the maximum diameter measured experimentally. As an example, let us say we have a patient with six consecutive scans and want to predict the maximum diameter at the 4<sup>th</sup> scan. Then, the known data set is  $DC=\{t_1, t_2, t_3\}$  and the “true” diameter to be predicted is  $DV=t_4$ , in other words, the DV is the ground truth for the QoI. The performance of the predictive model at each particular QoI was assessed independently, because an acceptable performance at a specific QoI does not necessarily imply reasonable performance for all possible QoI.

All model parameters with vector  $\theta = (\theta_1, \theta_2, \dots, \theta_d) \in \mathbb{R}^d$  treating as a vector of random variables  $\theta: \Omega \rightarrow \mathbb{R}^d$ , where  $\Omega$  denotes a suitable sample space. The numerical algorithms were applied to calibrate the exponential AAA growth model, given in Equation 4, against a subset of the experimental data. The criteria were determined to assess the convergence of the algorithm.

### Calibration model

We used a Bayesian approach, which fundamentally enhances our subjective belief by the probability of an event via incorporation of population clinical data, to update the prediction of AAA diameter growth. We followed the notation and terminology introduced by Gelman et al. [31]. A set of calibration parameters were denoted by  $\theta$  and the observed data were denoted by  $y=\{y_1, y_2, \dots, y_n\}$ . Furthermore, the marginal and conditional probability of density function (pdf) were donated by  $p(\cdot)$  and  $p(\cdot|\cdot)$ ,

respectively. In our AAA growth model,  $\theta$  corresponds to the model parameters in Equation 4 (i.e.,  $\theta_1 = \alpha$  and  $\theta_2 = \beta$ ) and  $y$  corresponds to the maximum spherical diameter at the time points in the calibration data set SC. The observable outputs in the prediction model are, thus, related to the input parameters by

$$\mathbf{y} = D(t; \boldsymbol{\theta}, \mathbf{e}) \quad (5)$$

where  $D$  and  $e$  respectively corresponds to the maximum spherical diameter and the measurement error. The relationship between the maximum spherical diameters (observable outputs) and model inputs at time  $t$  can be formulated by

$$\mathbf{y} = D(t; \boldsymbol{\theta}) + \boldsymbol{\delta}(t) + \boldsymbol{\varepsilon} \quad (6)$$

where  $\boldsymbol{\varepsilon}$  corresponds to error, the diameter  $D(\cdot; \cdot)$  can be viewed as a function of  $t$  and  $\boldsymbol{\theta}(\alpha, \beta)$ , and  $\boldsymbol{\delta}(t)$  corresponds to a discrepancy function. However, we ignored here to systematic model discrepancies explicitly by following the methodologies referred by Kennedy et al. [32], Higdon et al. [33] and Bayarri et al. [34]. As a result, a calibration model related to AAA growth outputs were given by;

$$\mathbf{y} = D(t; \boldsymbol{\theta}) + \boldsymbol{\varepsilon}. \quad (7)$$

## Bayesian inference and prediction

### *Statistical Model*

The joint pdf denoted by  $P_{JOINT}(\boldsymbol{\theta}, \mathbf{y})$  can be formulated by the product of the prior distribution of  $\boldsymbol{\theta}$ , denoted by  $P_{PRIOR}(\boldsymbol{\theta})$  and the sampling distribution denoted by  $P_{SAMPLE}(\mathbf{y}|\boldsymbol{\theta})$  as following

$$P_{JOINT}(\boldsymbol{\theta}, \mathbf{y}) = P_{PRIOR}(\boldsymbol{\theta})P_{SAMPLE}(\mathbf{y}|\boldsymbol{\theta}). \quad (8)$$

The conditional probability assigned to the parameters, which is posterior density, can be obtained by Bayes's theorem

$$P_{POST}(\boldsymbol{\theta}|\mathbf{y}) = P_{PRIOR}(\boldsymbol{\theta}) \frac{P_{SAMPLE}(\mathbf{y}|\boldsymbol{\theta})}{P_{PRIOR}^{PRED}(\mathbf{y})}, \quad (9)$$

where  $P_{PRIOR}^{PRED}(\mathbf{y})$  denotes the marginal distribution, which is averaging the likelihood over all possible parameter values with respect to the prior density.

$$P_{PRIOR}^{PRED}(\mathbf{y}) = \int P_{PRIOR}(\boldsymbol{\theta})P_{SAMPLE}(\mathbf{y}|\boldsymbol{\theta})d\boldsymbol{\theta}. \quad (10)$$

The density of  $P_{SAMPLE}(\mathbf{y}|\boldsymbol{\theta})$ , a function of  $\boldsymbol{\theta}$  rather than  $\mathbf{y}$ , is called likelihood function and interpreted as how likely a parameter value is, given a particular outcome. The subjective beliefs in the values of the parameters before the measurement was made denoted by  $P_{PRIOR}(\boldsymbol{\theta})$ . Thus, a posterior distribution denoted by  $P_{POST}(\boldsymbol{\theta}|\mathbf{y})$  can be considered as an enhanced degree of belief, which is obtained with incorporation of the experimental data.

### *Selection of Prior Distribution*

The posterior distribution of the population was served as the prior for both growth prediction models, Patient-Oriented Growth Prediction Model (POGPM) and Generalized Linear Model (GLM) enhanced POGPM. The methodology finding the Posterior Distribution of Population (PDoP) for a spherical diameter, which is used in POGPM explained here. The same approach was also followed to estimate the parameters for a tortuosity measurement, which is used in GLM enhanced POGPM with a spherical diameter measurement together.

The prior distributions of  $\alpha$  and  $\beta$  are assumed to be normally distributed random variables with parameters (mean and deviation). The prior of  $\alpha$ , an initial diameter at time  $t=0$ , was set at mean 30 mm because AAA is clinically defined as an enlargement of the abdominal aorta to  $>3.0$  cm [1] and deviation 2 mm because the absolute intra-observer difference of the maximum diameter was 2 mm [35], respectively. The prior of  $\beta$  (the growth rate) is set at mean 0.004 and variance 0.001 based on statistical characteristics of aneurysm growth [14]. Although the base distributions used in the common (population) model was Gaussian, Student's t-test distribution was used in the patient specific model because the number of observations for a single patient is too small to support a Gaussian. Student's t-distribution, on the other hand, can be applied as the POGPM since it is designed to be less concentrated around its peak and has heavier tails as the degree of freedom decreases, thus better capturing the level of uncertainty given less evidence, especially with respect to extreme observations. The more evidence we have per patient, the more this distribution will approximate a Gaussian.

The pre-assumed values for the mean of the prior distribution are updated using the Maximum A Posteriori (MAP) method based on the aforementioned data. A version of the Expectation-Maximization algorithm is used to find the most likely parameters: First, an initial growth curve, a function of  $\alpha$  and  $\beta$  in **Equation 4**, is chosen and patients' scans are time-shifted based on the measurements at the first observed scans. Then, the MAP estimate is made to update the predictors of the growth curve and find a better fit function. The shifting and MAP estimation steps are iteratively repeated until the likelihood converges (i.e. total amount of error no longer decreases). As a result, the best fit of the growth curve, namely the master curve, is found.

### *Selection of Likelihood*

The likelihood function for the parameter  $\theta$ , given data  $\mathbf{y}$ , were specified to determine how the biological AAA growth model and experimental data  $\mathbf{y}$  inform the posterior distribution. The measurement error of the maximum diameter at each time point were assumed to be independent and the processes determining the true diameter are deterministic. Furthermore, the experimental noise is normally distributed about 0 with variance  $\sigma_D(t)$ , which denotes  $\sigma_D$  at time  $t$ . Under these assumptions, the likelihood is formulated by

$$P_{SAMPLE}(\mathbf{y}|\theta) = \prod_{i \in S_C} \frac{1}{\sqrt{2\pi\sigma_V^2(t_i)}} \exp\left(-\frac{(y_i - D(t_i; \theta))^2}{2\sigma_V^2(t_i)}\right). \quad (11)$$

### *Sampling of Posterior Distribution*

Obtaining the posterior distribution is analytically possible when a certain combination of prior distribution and likelihood have met; in general, this is not the case. Numerical approach, drawn sample from the posterior distribution  $P_{POST}(\theta|\mathbf{y})$  via a discrete approximation are often required to be used for this purpose. Hawkins-Daarud et al. [30] and Gelman et al. [31] proposed a solution to drawn sample from the posterior distribution using a regular grid in the parameter space. However, this has a computational cost especially for the complex model if it has a lot of inferred parameters. Instead, we applied a well-known method, Markov Chain Monte Carlo (MCMC), sampling for posterior distribution in this study.

There are examples of random walk Monte Carlo methods as a kind of random simulation available in literature. Metropolis-Hastings algorithm is the very first, and simpler than MCMC, and commonly used in literature. However, the algorithm works by performing a random walk that takes a lot of computational time and, furthermore is sensitive to the selection of a suitable proposal distribution. Therefore, we deemed it not very suitable for our moderately complex case. Gibbs sampling is a popular example of random walk because it does not require any such tuning. However, Gibbs sampling, again, is not the most efficient (computationally speaking) approach and was not employed here.

To avoid the computational inefficiency of a random walk and the requirement to tune the proposal distribution, especially given the high-dimensional target distribution in question, we decided on the Hamiltonian Monte Carlo (HMC) algorithm (or Hybrid Monte Carlo), which is a Markov Chain Monte Carlo method for obtaining a sequence of random samples. Therefore, No-U-Turn Sampler (NUTS), an extension to HMC method, was used with no hand-tuning in this study [20].

Probabilistic programming is an approach that uses automatic Bayesian inference on a user-defined probabilistic model with the help of MCMC sampling, and is therefore used to perform inference and parameter estimation on arbitrarily complex probabilistic graphical models. In this study, PyMC3 [36], an open source probabilistic programming framework written in Python, was used in POGPM and GLM enhanced POGPM. PyMC3 was preferred as it is a commonly used framework, with good community support, featuring an optimized inference engine based on likelihood gradient convergence, as well as a number of common distributions, such as Beta, Gamma, Binomial and Categorical, where the values of the parameters determine the location, shape or scale of the randomly generated numbers depending on the specific parameterization of the distribution.

### 3.3.2. Patient-oriented Growth Prediction Model (POGPM)

The biological of AAA growth model was fully specified by formulating mathematically AAA growth, experimental data and the QoI for predicting the future diameter using the calibrated growth model. The Bayes framework is applied for predicting patient-oriented growth, as summarized in Figure 5. In this study, a two-system approach based on Bayesian calibration [24] was used and the aneurysm growth model was specified according to individual patient characteristics.

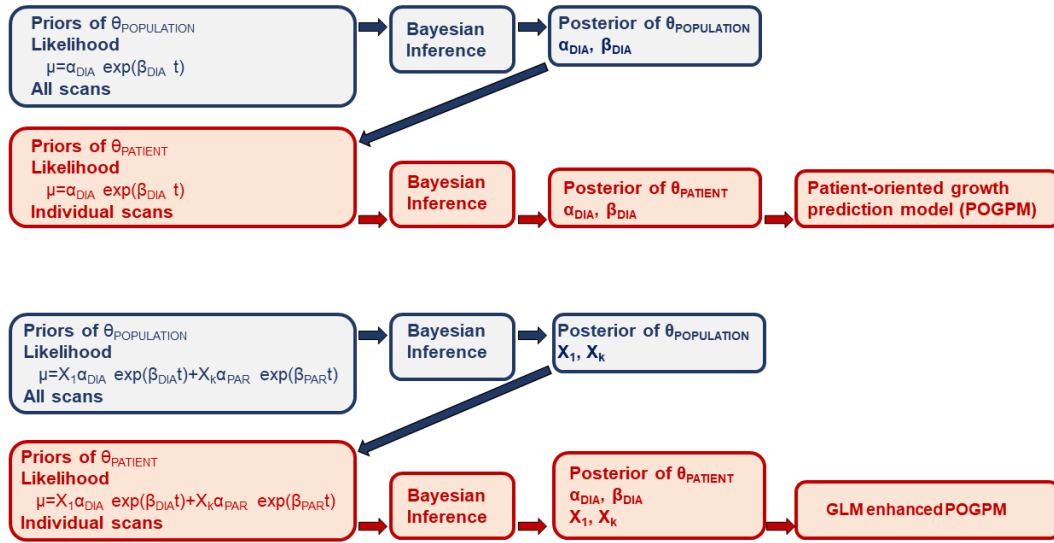


Figure 5. The work-flow diagrams for POGPM (top) and GLM enhanced POGPM (bottom)

The parameters of PDoP were estimated using the spherical diameter based on the whole population. The POGPM is specified according to each patient separately, since each patient has different characteristics and their growth rate was different. In that case, the posterior distribution from the population model (i.e. common for Korean

patients) was set and fed to POGPM as the prior for each patient's specific model by using Bayesian two-stage model [24]. Once a patient specific model is thus built, the prediction of a measurement at any future time-point can be made, along with an estimate of the uncertainty associated with the prediction.

### 3.3.3. Generalized Linear Model (GLM) enhanced POGPM

Although, the POGPM can accurately predict follow-up diameter in the majority of cases, in some scans, sudden increases or decreases were observed. The commonalities between these scans were analyzed. First, all the scans were categorized based on their baseline spherical diameter into three classes, namely 'over-estimated', 'under-estimated' and 'within tolerance'. Then, all geometric measurements belonging to the three groups were analyzed separately using pairwise t-tests to reveal if there was a significant ( $\alpha=0.05$ ) predictor for sudden diameter growth.

In addition to spherical diameter, the study was extended using the Generalized Linear Model (GLM) with Bayesian inference to take significant features into account. Each pair of geometric properties was analyzed in terms of their correlations and if two features were highly correlated ( $\text{corr} > 0.9$ ), one of the two was dropped, because features with high correlation have almost the same effect on the dependent variable. For example, perimeter is strongly correlated with diameter ( $\text{corr}=0.93$ ) and was removed from the feature set. Furthermore, the optimal model was built with only statistically significant variables ( $p < 0.05$ ). Different features were removed and p-values in each case were measured in order to decide whether to keep a feature or not. Thus, additional geometrical parameters, denoted by PAR, were selected based on p-values using Backward Elimination.

$$\text{Growth} \sim X_1 \text{MAX}_{\text{DIA}_S} + X_k \text{PAR}, \quad (12)$$

where PAR is an additional geometrical parameter. The growth is a function of the posterior distribution of both spherical diameter ( $\text{MAX}_{\text{DIA}_S}$ ) and PAR while X are the coefficients. The PDoP for PAR was found by following the same approach, which was already explained, to find PDoP for  $\text{MAX}_{\text{DIA}_S}$ . The parameters of coefficients of the population (mean and standard deviation), unknown parameters in **Equation 12**, were then found using the GLM model, and were set as priors. These PDoPs, which were already specified for  $\text{MAX}_{\text{DIA}_S}$  and PAR according to observations made on the CT scans belonging to a particular patient, were used to subsequently predict aneurysm follow-up diameter based on time.





## CHAPTER 4

### RESULTS

This chapter briefly presented the results related to this study. The obtained results are laid out in two main sections: (1) correlation analyses and defining master curve of AAA growth; and (2) probabilistic programming for patient-oriented AAA growth.

#### 4.1. Correlation Analyses and Defining master curve of AAA growth

All geometrical measurements describing the geometric properties of each scan were calculated. First, these measurements were analyzed in terms of their correlations regardless of time interval between consecutive scans. Second, the growth rate of each measurement was computed by considering changes in parameters between two consecutive scans. Finally, growth curves, namely master curves, were constructed for these measurements to evaluate prediction accuracy. All these results were sequentially given under proper titles below.

##### 4.1.1. Maximum measurements for correlation analysis

A total of 21 measurements were analyzed in terms of their correlations for each observation and are summarized in **Table 3**. The correlation study showed that AAA volume is highly correlated with diameter, regardless of method used to calculate the maximum diameter (spherical ( $r=0.89$ ), axial ( $r=0.91$ ) or orthogonal ( $r=0.92$ )). Similarly, very high correlations were found between the diameters and perimeters regardless of methods used ( $r>0.92$ ). All primary parameters ( $r=0.69$  and  $0.77$ ) are mildly correlated with ILT volume. However, the secondary parameters are significantly less correlated with the primary parameters, except ILT volume. For instance, eccentricity ( $r=0.60$ ) and tortuosity ( $r=0.55$ ) are moderately correlated with AAA volume; only maximum ILT thickness ( $r=0.52-0.59$ ) is moderately correlated with maximum diameter measurements.

Table 3. Correlations of geometrical parameters on AAA actual measurements

	Parameters	VOL <sub>AAA</sub>	VOL <sub>ILT</sub>	MAX <sub>DIA_S</sub>	MAX <sub>DIA_O</sub>	MAX <sub>DIA_A</sub>	MAX <sub>PER_O</sub>	MAX <sub>PER_A</sub>
1°	VOL <sub>AAA</sub>	1						
	MAX <sub>DIA_S</sub>	<b>0.89</b>	0.69	1				
	MAX <sub>DIA_O</sub>	<b>0.92</b>	0.72	<b>0.92</b>	1			
	MAX <sub>DIA_A</sub>	<b>0.91</b>	<b>0.77</b>	<b>0.94</b>	<b>0.95</b>	1		
	MAX <sub>PER_O</sub>	<b>0.93</b>	0.74	<b>0.96</b>	<b>0.96</b>	<b>0.96</b>	1	
	MAX <sub>PER_A</sub>	<b>0.92</b>	<b>0.75</b>	<b>0.93</b>	<b>0.92</b>	<b>0.94</b>	<b>0.94</b>	1
2°	VOL <sub>ILT</sub>	<b>0.78</b>	1					
	MAX <sub>ECC_O</sub>	0.60	0.08	0.22	0.47	0.33	0.28	0.30
	TORT_CL	0.55	-0.16	0.04	0.07	0.01	0.03	0.03
	MAX <sub>ILT</sub>	0.46	<b>0.81</b>	0.53	0.52	0.59	0.56	0.59
	A <sub>ILT</sub>	0.35	0.70	0.39	0.42	0.47	0.42	0.49

#### 4.1.2. Growth rates and correlation analysis

Growth rates using the maximum spherical (median 6.04%/year, IQR 5.66%/year), orthogonal (median 6.47%/year, IQR 7.14%/year), and axial (median 5.75%/year, IQR 5.95%/year) diameters, as well as aneurysm volumes (median 13.44%/year, IQR 15.12%/year) are depicted in Figure 6. The normality of the diameters and the aneurysm volume growth were analyzed using the Shapiro-Wilk test, and the result confirmed the normality of the diameters (spherical  $p=0.87$ , axial  $p=0.27$  and orthogonal  $p=0.53$ ) but not the volume ( $p=0.01$ ). A Mann Whitney U test indicated that the diameters were not significantly different from each other ( $p>0.77$ ). However, the growth rates of these diameters were significantly different from that of the aneurysm volume ( $p<0.01$ ).

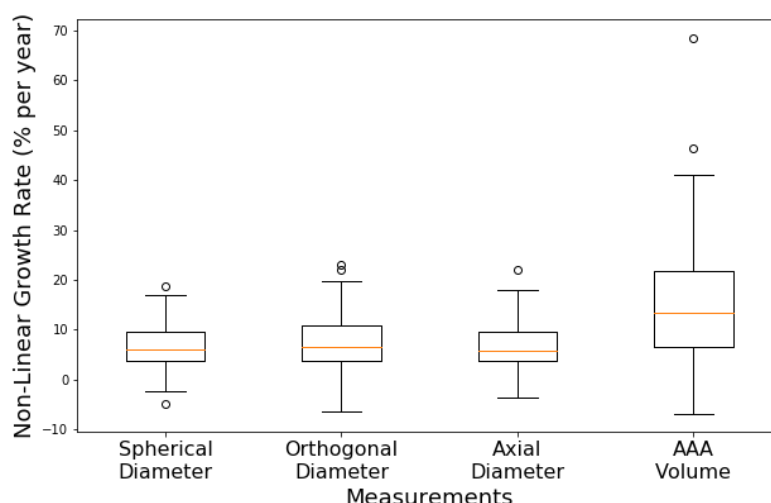


Figure 6. Box and whisker plots for the growth rate of the diameters and aneurysm volume using non-linear model

In addition, the growth rate for each measurement was calculated in a non-linear fashion and their pairwise correlation was analyzed in **Table 4**. AAA volume expansion rates are highly correlated with axial diameter growth rates ( $r=0.80$ ), and moderately correlated with the spherical ( $r=0.61$ ) and orthogonal ( $r=0.72$ ) diameter growth rates. Orthogonal and axial diameter growth rates have a strong correlation with each other ( $r=0.78$ ), whereas these two rates do not show a strong correlation with spherical diameter growth rates ( $r=0.55$  and  $0.67$ , respectively).

Table 4. Correlations of geometrical parameter rates of change on AAA measurements using non-linear growth model

	Parameters	VOL <sub>AAA</sub>	MAX <sub>DIA_S</sub>	MAX <sub>DIA_O</sub>	MAX <sub>DIA_A</sub>	MAX <sub>PER_O</sub>	MAX <sub>PER_A</sub>
1°	VOL <sub>AAA</sub>	1					
	MAX <sub>DIA_S</sub>	0.61	1				
	MAX <sub>DIA_O</sub>	0.72	0.55	1			
	MAX <sub>DIA_A</sub>	0.80	0.67	0.78	1		
	MAX <sub>PER_O</sub>	0.78	0.75	0.90	0.78	1	
	MAX <sub>PER_A</sub>	0.81	0.77	0.83	0.90	0.94	1
2°	VOL <sub>ILT</sub>	0.80					
	MAX <sub>ECC_O</sub>	0.09	0.13	0.17	0.07	0.15	0.13
	TORT_CL	0.13	0.09	0.12	-0.02	0.09	0.07
	MAX <sub>ILT</sub>	0.53	0.42	0.44	0.55	0.44	0.48
	A <sub>ILT</sub>	0.12	0.26	0.28	0.19	0.26	0.30

AAA volume expansion rate is highly correlated ( $r=0.80$ ) with thrombus accumulation rate. However, the aneurysm volume expansion rate is not highly correlated with the maximum ILT thickness ( $r=0.53$ ) nor with the lumen volume ( $r=0.45$ ) rates. Other secondary parameters such as eccentricity, tortuosity, ILT thickness and area fraction rates are not highly correlated with AAA volumetric expansion rates ( $r=0.09$ ,  $0.13$ ,  $0.53$  and  $0.12$  respectively). Additionally, eccentricity and tortuosity parameters are not correlated with any of the primary parameters ( $r<0.17$ ).

#### 4.1.3. Growth curve of the geometric measurements

Growth curves were constructed for the measurements in order to find one that could predict aneurysmal growth. Figure 7 compares the master curves obtained for maximum spherical diameter (left) and orthogonal diameter (right). The best three representatives of the master curves were selected based on their r-square scores. The spherical diameter (MAX<sub>DIA\_S</sub>) was found to be the best growth representative (r-square: 0.985) and the three next-best representatives were MAX<sub>PER\_A</sub> (0.977), DIA<sub>PER\_A</sub> (0.972), and MAX<sub>DIA\_O</sub> (0.970). Figure 8 shows the prediction of AAA growth based on the master curve and the histogram of error prediction, based on spherical diameter.

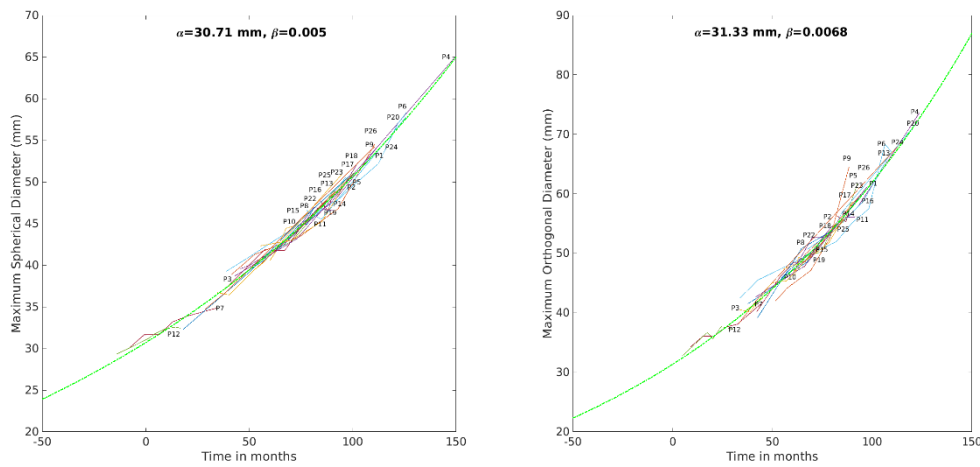


Figure 7. The exponential functions of maximum spherical diameter (left) and maximum orthogonal diameter (right). The spherical diameter is the best representative of AAA growth

Using the master curve function derived (mean=0.24 mm, sigma=2.10 mm), the spherical diameter was correctly predicted to 74 of 79 scans (visualized by blue lines Figure 8a), based on a 95% confidence interval. Similarly, the prediction capabilities of other diameter measurements were found to have averages of 0.52 mm and 0.08 mm, and standard deviations of and 3.23 mm and 2.68 mm, for orthogonal and axial, respectively.

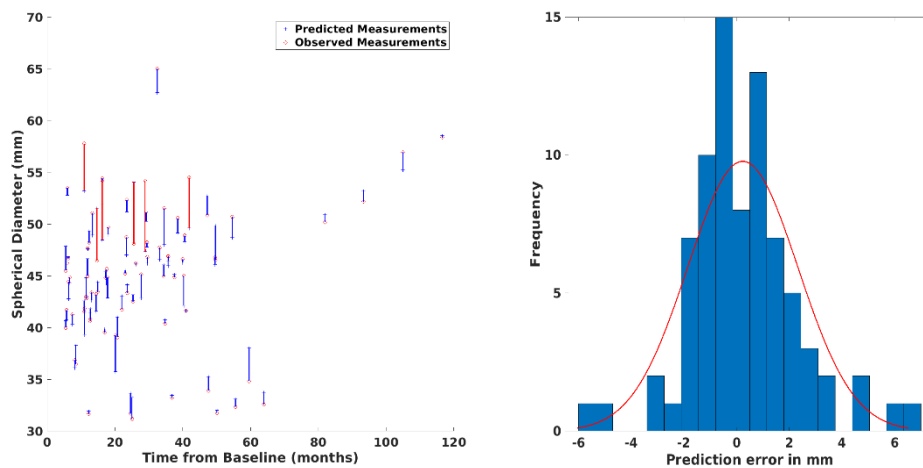


Figure 8. The prediction of AAA growth based on the master curve (spherical diameter). a) The actual and predicted values are plotted with respect to time from baseline. b) The histogram of prediction errors and estimation of normal distribution parameters

## 4.2. Probabilistic Programming for Patient-Oriented AAA Growth

The master growth curve over the time does not necessarily follow the common pattern for all patients, each patient having different characteristics, accuracy suffered for patients having relatively faster or slower AAA growth. This study also developed an enhanced prediction growth model applicable for predicting AAA growth accurately using Bayesian inference. An exponential growth model was built specifically on patient characteristics.

### 4.2.1. Posterior distribution of population (PDoP)

Bayesian calibration using the exponential function for 25 AAA patients with 106 CT scan images estimated the parameters of PDoP, which were served for prior distribution of predictors for both the baseline diameter and the diameter growth rate.

The estimated parameters of population posterior distribution using the spherical diameter are demonstrated in Figure 9. There are two parameters being estimated: the baseline diameter  $\alpha$  (mean=32.06 mm, sigma=0.55 mm) and exponent of the growth rate  $\beta$  (mean=0.0043, sigma=0.0002). The parameters of the growth prediction model,  $\alpha$  and  $\beta$ , are specified based on this fit.

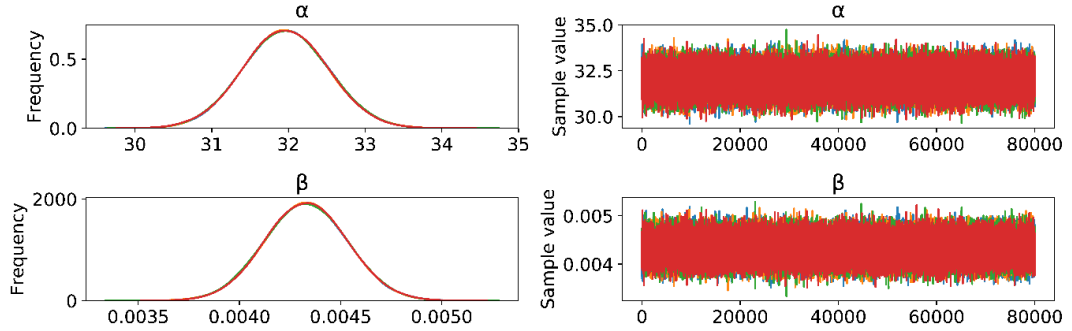


Figure 9. The frequencies of estimated parameters for the PDoP growth model ( $\alpha$  and  $\beta$ ) and parameter values from drawn samples

The characteristics of the population growth were analyzed using different forms of distributions such as normal z and student t test. The posterior distributions of the stochastic values were found almost the same for both z and t distribution because the number of samples ( $n=105$ ) is so sufficient that t distribution ( $\alpha \sim N(31.897889, 0.543275)$ ,  $\beta \sim N(0.004350, 0.000202)$ ) approximates the z distribution ( $\alpha \sim N(32.063321, 0.549830)$ ,  $\beta \sim N(0.004299, 0.000201)$ ). Figure 10 represents the normal distribution of the samples drawn from the specified model. The average and standard deviation of the follow-up diameter for the population is 43.41 mm and 7.05 mm.

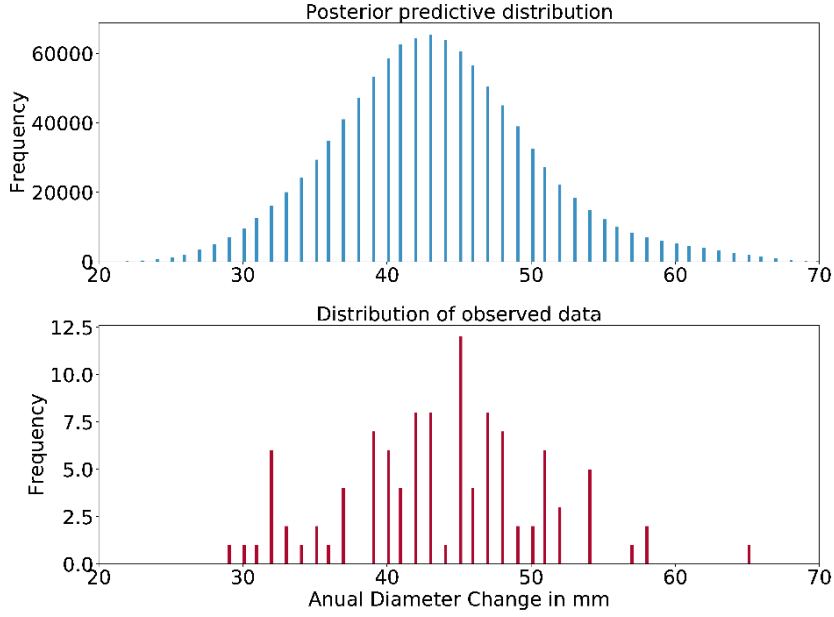


Figure 10. The estimated parameters of the posterior distribution of the drawn samples for the Korean population(up) and the distribution of observed scans (down)

The PDoP has growth model of two predictor variables;  $\alpha$  and  $\beta$ , were normally distributed random variables with parameters  $\alpha \sim N(32.063, 0.5498)$ ;  $\beta \sim N(0.0043, 0.0002)$  respectively. Based on the mean of posterior distribution, aneurysm growth for the next diameter at any time using can be predicted by Equation 13 and Equation 14:

$$T = \ln(D^{baseline} \div 32.063) \div 0.0043, \quad (13)$$

$$D^{follow-up} = 32.063 * e^{(0.0043 * (t+T))}, \quad (14)$$

where  $D^{baseline}$  describes the diameter at the baseline scan,  $T$  represents how many months have passed once the aneurysm was observed and  $t$  determines the period of time in months for the next prediction.

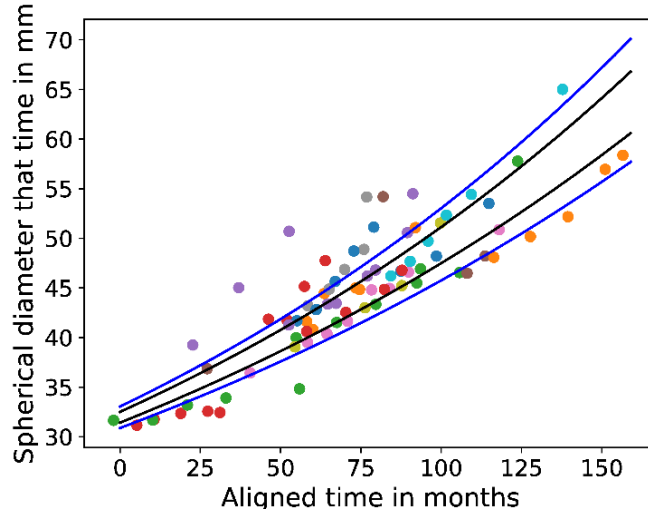


Figure 11. The observed scans and aneurysm growth model based on the estimated parameters of PDoP and time interval between consecutive scans with 0.68 and 0.95 prediction interval. The aligned time is the shared time axis for all the patients. Since the AAA stages of the patients at the time of first scan were not the same, the time of the scan must be shifted in the shared time axis. The follow-up diameters of the 81 CT scans from 25 patients are marked on the plot with dots, where each color indicates an individual patient. Since the first scan of each patient was known, only follow-up scans (81 of 106 scans) that were QoIs in prediction, are presented in the graph.

Figure 11 shows that the follow-up diameter was correctly predicted to within 2.7 mm error in 64 of 81 scans (79%) using the PDoP based on a 95% confidence interval. There are, however, 17 of 21 scans (21%) which were not followed the common properties of the population. The number of CT scans for which the growth rates are over- and under-estimated are 4 of 17 (24%) and 13 of 17 (76%) respectively.

#### 4.2.2. Patient-oriented prediction of AAA growth

An individual POGPM (Patient Oriented Growth Prediction Model) was specified according to the patient growth characteristics, where a patient was selected with a number of consecutive scans. Figure 12 is an example of a POGPM constructed for patient 11 and patient 23, using the obtained scans, which were the stochastic observations, and the posterior distribution of the unknown parameters for the population using the workflow of POGPM (Figure 5), i.e., using the prior distribution from the PDoP.

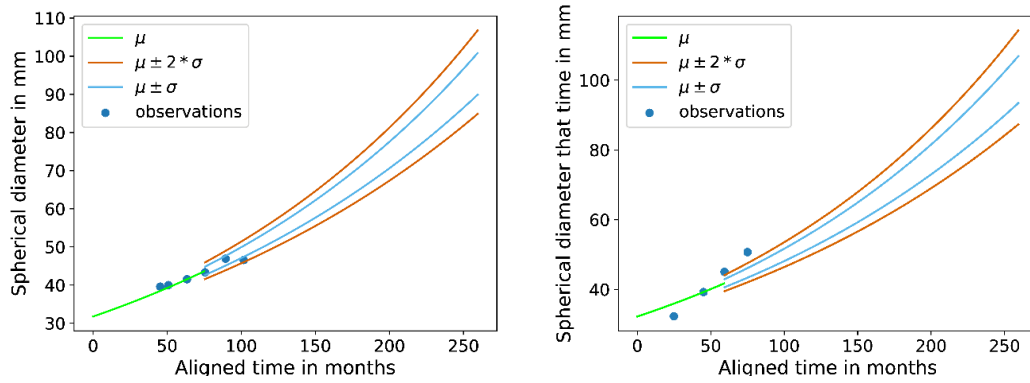


Figure 12. An example of the demonstration for the prediction capability of a POGPM at 77th months (4th observed scans of patient with id 11) and at 59th months (3rd observed scans of patient with id 23) with confidence 0.68 and 0.95 intervals. The time was aligned according to population growth curve. All previously obtained measurements for a patient were used for predicting the measurement at the next scan.

The mean, standard deviation and the degree of freedom of the posterior distribution (estimated parameters of student-t distribution) at the 77<sup>th</sup> months were found 43.72 mm, 0.47 mm and 1.81, respectively. Similarly, all these parameters of the distribution were estimated since from the 4<sup>th</sup> scan observed, and both blue and orange lines were drawn in order to represent the upper and lower limit of the next prediction according to the time. In this example, the observed diameter of the patient 11 at the 4<sup>th</sup> scan is 43.34 mm. The observed diameters were predicted between 43.05 and 44.39 mm with 0.68 confidence level ( $p=0.32$ ) and 41.50 and 45.94 mm with 0.95 confidence ( $p=0.05$ ). The figure also shows that the last CT scan of the patient was outside of the prediction range with 0.68 confidence. However, the growth model would be updated using the stochastic observation for 4<sup>th</sup> and 5<sup>th</sup> CT scans and the prediction range would be changed accordingly. This is an example of successful model constructed according to the patient first 3<sup>rd</sup> observed scans (characteristics), because the observed diameter was found inside the limit of prediction range with both 0.68 and 0.95 confidence levels.

The observed diameter of the patient 23 at the 3<sup>rd</sup> scan is 45.02 mm. However, the observed diameters were predicted between 39.44 and 43.90 mm with 0.95 confidence if PDoP, the posterior distribution of Korean population, was used. As Figure 12 demonstrates, the observed diameter was outside of the prediction range, and this patient does not follow the common growth model of the population. This is an example of underestimated scans using PDoP, were accurately modeled within tolerance, if the GLM enhanced POGPM which has both the capability of taking into a patient individual characteristics and other geometry account was used. The observed diameter was found inside the limit of prediction range (between 40.12 and 45.09 mm) with 0.95 confidence levels.



The growth model using a diameter provided different results for posterior distributions specified by the characteristics of patient and population as **Table 7** shows. The percentage of observed scans, accurately model in population and patient oriented growth, are respectively 79 (n=64) and 83 (n=67) specified with .95 confidences (p=0.05). The average error in mm were  $\pm 2.67$  mm and  $\pm 2.61$  mm respectively. Furthermore, 88% and 64% of scans were accurately model in POGPM at 1<sup>th</sup> and 2<sup>nd</sup> year, respectively.

#### 4.2.3. Enhanced prediction of AAA growth

The aneurysm growth could not be successfully modeled for some scans using only diameter. For example, the diameter of Patient 23 at the 3rd scan, was predicted between 39.13 and 44.1 mm with prediction intervals of 0.95 as demonstrated by Figure 12. However, the observed diameter was 45.02 mm. Thus, the other geometric measurements were considered to help explain such unexpected change in the growth and to decrease the number of such inaccurate observations.

Table 5. The mean and standard deviation of each category, and their paired t-test results.

		<b>A<sub>ILT</sub></b>	<b>MAX<sub>ILT</sub></b>	<b>VOL<sub>LUMEN</sub></b>	<b>MAX<sub>ECC_O</sub></b>	<b>MIN<sub>DIA_O</sub></b>	<b>TORT_CL</b>
<b>Under-estimated Scans (U) n=10</b>	<b>mean</b>	0.35	13.04	62019.15	1.40	17.92	1.19
	<b>sd</b>	0.22	4.00	16077.36	0.27	4.06	0.12
<b>Over-estimated Scans (O) n=4</b>	<b>mean</b>	0.26	10.50	59352.61	1.24	19.58	1.12
	<b>sd</b>	0.22	6.41	9093.67	0.04	2.35	0.05
<b>Within Tolerance Scans (T) n=67</b>	<b>mean</b>	0.30	13.92	61669.42	1.34	19.14	1.10
	<b>sd</b>	0.17	6.86	16930.94	0.23	2.96	0.06
<b>T-Test Between Categories (p-values)</b>	<b>U-T</b>	0.3747	0.6952	0.9513	0.4247	0.2511	<b>0.0002</b>
	<b>T-O</b>	0.6755	0.3357	0.7879	0.4112	0.7743	0.5114

The common properties of the baseline scans were analyzed by taken into all other geometrical measurements account; and the average and standard deviation of each categories (under-estimated, over-estimated and within tolerance scans) were summarized in **Table 5**. The inter-variance between categories were analyzed using the t-test (two tailed, equal variance) and the tortuosity of centerline among the all considered geometrical measurements were found significant (p=0.0002) for the

categories of under-estimated and within tolerance scans. In the GLM enhanced POGPM for Equation 12, PAR is replaced by the parameter, TORT\_CL.

Although the number of patients used in the study is 25, there are 81 CT scans which were analyzed using a pairwise t-test. Therefore, we believe this is a sufficient number of subjects that the result is statistically significant. A p-value less than 0.05 (typically  $\leq 0.05$ ) was considered statistically significant in this study. Additionally, power analysis for two-group independent sample t-test was applied, with significance level (alpha) and power assumed as default at 0.05 and 0.8, respectively. The calculation results indicate that we need to have a total sample size of 56 subjects (we had 81 CT scans). We also applied Analysis of Variance (ANOVA) one-way test to all three groups and found that only the tortuosity of centerline was significant. The results were demonstrated in the following table.

Table 6. The mean and standard deviation of each category, and their paired t-test results.

		A <sub>ILT</sub>	MAX <sub>ILT</sub>	VOL <sub>LUMEN</sub>	MAX <sub>ECC_O</sub>	MIN <sub>DIA_O</sub>	TORT_CL
<b>Under-estimated Scans (U)</b> n=10	<b>mean</b>	0.35	13.04	62019.15	1.40	17.92	1.19
	<b>sd</b>	0.22	4.00	16077.36	0.27	4.06	0.12
<b>Over-estimated Scans (O)</b> n=4	<b>mean</b>	0.26	10.50	59352.61	1.24	19.58	1.12
	<b>sd</b>	0.22	6.41	9093.67	0.04	2.35	0.05
<b>Within Tolerance Scans (T)</b> n=67	<b>mean</b>	0.30	13.92	61669.42	1.34	19.14	1.10
	<b>sd</b>	0.17	6.86	16930.94	0.23	2.96	0.06
<b>T-Test Between Categories (p-values)</b>	<b>U-T</b>	0.3747	0.6952	0.9513	0.4247	0.2511	<b>0.0002</b>
	<b>T-O</b>	0.6755	0.3357	0.7879	0.4112	0.7743	0.5114
<b>Analysis of Variance (ANOVA)</b>	<b>p-values</b>	<b>0.63</b>	<b>0.57</b>	<b>0.96</b>	<b>0.495</b>	<b>0.475</b>	<b>0.001</b>

In addition to the diameter, the aneurysm growth was also modeled by considering the tortuosity of the centerline using GLM enhanced POGPM. The percentage of observed scans, accurately model in GLM enhanced POGPM was 86 (n=70) with .95 confidences (p=0.05), and the average error in mm was  $\pm 2.79$  mm as **Table 7** shows. Each pair of the average error of prediction growth models in mm was analyzed using pairwise t-test, and their differences were not found statistically significant ( $p > 0.05$ ). Furthermore, 93% and 64% of scans were accurately model in GLM enhanced

POGPM at 1<sup>th</sup> and 2<sup>nd</sup> year, respectively. The estimated parameters of posterior normal distribution of predictors and coefficients are as follows;  $\alpha_{DIAS} \sim N(32.063, 0.549)$ ,  $\beta_{DIAS} \sim N(0.0043, 0.0002)$ ,  $\alpha_{TORTCL} \sim N(1.012, 0.0047)$ ,  $\beta_{TORTCL} \sim N(0.0013, 0.00005)$ ,  $\theta_1 \sim N(1.023, 0.039)$ ,  $\theta_2 \sim N(-0.313, 1.532)$ ,  $\sigma \sim |N(0.0, 1.0)|$ ,  $\mu = \theta_1 * MAX_{DIAS} + \theta_2 * TORTCL$ , and  $Y \sim N(\mu, \sigma^2)$ .

Table 7. The percentage of scans accurately modeled using PDoP, the POGPM and GLM enhanced POGPM

	<b>Underestimated Scans</b>	<b>Overestimated Scans</b>	<b>Within Tolerance Scans</b>	<b>Error in mm</b>
<b>PDoP</b>	16% (n=13)	5% (n=4)	79% (n=64)	2.67
<b>POGPM</b>	12% (n=10)	5% (n=4)	83% (n=67)	2.61
<b>GLM enhanced POGPM</b>	9% (n=7)	5% (n=4)	86% (n=70)	2.79



## CHAPTER 5

### DISCUSSION

This chapter briefly discussed the obtained results related to this study. The discussions are laid out in two main sections: (1) defining master curve of AAA growth and its potential utility of clinical management; and (2) the prediction capability of the growth model.

#### **5.1. Defining master curve of AAA growth and its potential utility of clinical management**

The guideline for clinical AAA management based on single maximum diameter criterion has been challenged [9], [10], [33], [40], with more studies proposing that the growth rate is associated with AAA rupture [18], [33]. An augmented criterion, the maximum diameter  $> 5.5$  cm or annual growth rate  $> 1$  cm/year, has been proposed for surgical intervention [6], [7]. There is, however, scarcity of morphological studies using longitudinal CT scan images. Therefore, this work aimed to construct a larger database of morphological parameters and to enhance the predictability AAA growth for high-risk aneurysms.

Previous studies suggested that orthogonal diameter yields the measure closest to real AAA size, and is superior to axial diameter, which tends to overestimate the diameters [58], [59]. The orthogonal diameter measurement method, however, can be dependent on the construction of the centerline, which can cause high variability. For instance, an error of  $5^\circ$  in determining the orthogonal plane might lead to 15 mm of miscalculation in measuring maximum diameters [39]. To address this issue, this study utilized a method to reduce variability which semi-automatically generates the centerline using maximally inscribed spheres.

The morphology of aneurysms is important for patient monitoring [48], [60]–[62]. In these studies, the measurements describing the shape of the aneurysms (e.g., saccular, fusiform) were also obtained and its effect on the aneurysm development were investigated. Ruptured AAAs were observed to be more tortuous and have larger diameter asymmetry [63]. Additionally, the effect of surrounding tissue, including vertebral column and osteophytes, on AAA growth and geometrical changes in terms of the shape and curvature was demonstrated in a longitudinal follow-up study [19].

They found that the region of aneurysm interacting with the spine was flattened. Thus, surrounding tissues may also be an important parameter to model aneurysms. Apart from measurements, demographic information such as age may also be important because expansion rate tends to be more rapid over the age of 60 [64]. Several studies have reported that age and gender play a critical role in the widening of the aorta [8].

Previous studies [40], [58] proposed that the aneurysmal volume measurement served to better predict the development of AAA and rupture risk than the maximum diameter measurement. One of our main findings from the correlation analysis on our morphological parameters is, however, that the total volume is highly correlated with all primary parameters (maximum diameters, perimeter).

Meanwhile, there has been increasing evidence that growth rate is important for predicting high rupture risk [18], [33]. AAA volume expansion rates are only mildly correlated with the spherical ( $r=0.68$ ) and orthogonal growth rates ( $r=0.67$ ). Furthermore, spherical diameter growth rates do not show strong correlations with axial and orthogonal diameter growth rates ( $r=0.55$  and  $0.72$ , respectively). Although the utilities of different maximum diameter measurements and their rates were not fully tested, Gharahi et al. [39], suggested that different diameter measurements may serve different purposes. In particular, the axial diameter measurement is conveniently determined without finding a centerline [58], orthogonal diameter is important for representing the actual size and assessing the rupture potential [58], [59], and the spherical diameter is potentially suitable for predicting the AAA growth.

AAA volume expansion rate is highly correlated ( $r=0.80$ ) with thrombus accumulation rate. Zambrano et al [65] demonstrated that ILT was initially formed at the region of aorta where low wall shear stress was observed and its accumulation rate was associated with the aneurysm's expansion rate. Similarly, Parr et al. [61] found that the aneurysm volume was correlated with thrombus volume and diameter. The secondary parameters such as eccentricity, tortuosity, area fraction covered by ILT, ILT thickness, and lumen volume present no strong correlation with AAA volume expansion in terms of geometrical (static) ( $r < 0.45$ ) and rate measurements ( $r < 0.50$ ). These parameters, however, might be still important for the assessment of rupture risk. In fact, previous studies reported that some parameters such as asymmetry and tortuosity [63], and ratio of ILT to AAA volume [62] are associated with rupture risk.

We used an exponential function [2], [40], [41] for modeling AAA growth since AAAs of 3-3.9 cm size expand slowly (a mean growth rate of 2.84 mm/year) compared to AAAs of 4-4.9 cm size (a mean growth rate of 3.66 mm/year). Similarly, previous studies reported growth rates of 1.1-7 mm/year for AAAs with 3-3.9 cm initial diameter, in contrast to the growth rate of 3-6.9 mm/year for AAA with 4-4.9 cm [66]. In addition to the growth rate studies, we analyzed the outcomes according to the expansion pattern. It was observed that an AAA with a 3 cm diameter will need surgical repair within the first 7 years of the scan. However, an AAA with a 4 cm diameter will reach 5.5 cm in the first 3 years. The UK SAT demonstrated that less than 20% of patients with 3-3.9 cm AAA would need surgical repair in the first 5 years

of follow-up [36], [67]. In the ADAM study, 27% of 4-5.5 cm AAA undergo surgical intervention in the first 2 years of follow-up [68]. The recent AAA guideline (2019) recommended safe surveillance intervals such as every three years for aneurysms 3–3.9 cm in diameter, annually for aneurysms 4.0–4.9 cm, and every 3–6 month for aneurysms  $\geq 5.0$  cm [3]. Therefore, the growth pattern computed in this follow-up study are consistent with those reported in the literature.

Most of all, this study found the spherical diameter as the best representative of the growth curve (r-square: 0.985) with a significantly higher prediction strength compared to other diameter measurements. Moreover, the maximally inscribed spheres method, minimizes the variability of the geometrical surface, and as a result, it leads to the least fluctuations and narrowest range in measurements [39].

We examined the utility of master curves and their prediction capabilities in terms of different geometrical parameters. The proposed model better predicts the growth of AAAs due to adopt an exponential growth function, rather than a traditional linear model, and systematically consider the effects of 21 geometric measurements (i.e. independent variables) on the growth rate. Among all the parameters, the master curve of spherical diameter performed best, predicting the diameter within 0.42 mm in 95% of all scans. In addition, we observed that the master curve using the spherical diameter resulted in the smallest prediction error ( $\sigma=2.10$  mm), while those of orthogonal and axial diameter resulted in larger errors ( $\sigma = 2.68$  mm and 3.22 mm). Therefore, we propose that a master curve for spherical diameter may be used as a clinical tool that gives insight about the future of aneurysm growth. This predictive tool can be used for planning for follow-up scans and surgical interventions.

## **5.2. The prediction capability of the growth model**

This study developed an enhanced prediction growth model applicable for predicting AAA growth accurately using Bayesian inference. An exponential growth model, commonly demonstrated in the previous studies, is selected and the estimated parameters of the posterior distributions, which were adopted from any observations (scans). This study used 106 CT scans from 25 patient dataset to construct PDoP and further predicts patient-specific AAA growth. Thus, the prediction of a measurement at any time-point can be made, along with an evaluation of the associated uncertainty.

The follow-up diameters can be predictable, if a patient follows the common growth model of the population. However, a rapid expansion of AAA, often associated with higher rupture risk, might be observed. For example, 23% ( $n=3$ ) of previously underestimated scans ( $n=13$ ), were accurately modeled within tolerance, if the POGPM was specified according to individual characteristics, while their errors in millimeters were almost the same. This is clinically important for monitoring the prognosis of aneurysm growth during the surveillance because the required immediate intervention based on the criteria defined by international guidelines might be

overlooked. Therefore, the aneurysm growth model was specified according to individual patient characteristics to predict the follow-up diameter for an AAA such a rapid growth was also observed. Additionally, the exponential growth model was enhanced by using other geometrical measurements. Thus, a tool having the improved potential of predicting AAA expansion or assessment of rupture risk, which is important in terms of elective surgical intervention and patient management, and applicable for anyone own observations to make prediction accurately, was developed. Therefore, Lee et al. [26] applied machine learning techniques for accurate prediction of AAA growth in an individual.

A patient-specific modeling of an AAA growth is an important step in terms of individualized diagnosis and clinical treatment. Zeinali-Davarani et al. used 3D geometry constructed from medical images and developed a computational framework for modeling AAA G&R [25]. In most studies of AAA biomechanics, the influence of the surrounding tissues was ignored [24]. This study, therefore, focused on further improvement of the G&R computational framework account for mechanical interaction between AAA and spine[24]. In addition to the prediction of an AAA, Zhang et al. also applied Bayesian calibration method to G&R computational model to quantify the associated uncertainty in the prediction [27].

In order to show the prediction performance of the model for the next measurement (in this case predicting what will be the 4th scan), we used the measurements of the 1st, 2nd and 3rd scans to specify the model and predicted only the next measurement. Even though the figure shows the measurements at the 5th and 6th scans, these measurements are given only for reference and are not used for evaluating the accuracy of the prediction of the 4th data point. If we want to predict the measurement at the 6th scan, all previous sequence of measurements (1st thru 5th scan) are used to specify the model according to patient characteristics. Actually, this approach is relevant for clinical use as the patient oriented growth model (the growth curve) is thus updated, as additional measurements are obtained. In summary, all previously obtained scans for a patient are used for predicting the subsequent scan.

One of the main strengths of this study is to have a relatively large number of scans analyzed. Although there exist previous papers using a physics-based computational modeling approaches for predicting AAA growth [18][19] and a study associated with uncertainty [27], the number of real observations was relatively small and no such assessment of the prediction model accuracy was available in their comparisons. Therefore, the results of our proposed solution could not be directly compared with these results, even though their approaches have similar advantages as Table 8, the state of the art comparison, shows.



Table 8. The state of the art comparison

Method	Motivation	Approach	Methods	Datasets	Uncertainty	Accuracy
Proposed model (POGPM)	prediction of future AAA growth	Two-stage Bayesian calibration	Probabilistic programming	106 CT scans	associated	83% of scans were predicted in 95% CI
Proposed model (GLM enhanced POGPM)	prediction of future AAA growth	Two-stage Bayesian calibration	Probabilistic programming	106 CT scans	associated	86% of scans were predicted in 95% CI
Farsad et al. (2015) [24]	trace to alteration of future AAA shape	G&R model	Finite Element Analysis	a few cases for demonstration	not capable	success demonstration on a few cases
Zeinali-Davarani et al. (2012) [25]	trace to alteration of future AAA shape	G&R model	Finite Element Analysis	a few cases for demonstration	not capable	success demonstration on a few cases
Zhang et al. (2019) [27]	trace to alteration of future AAA shape	Bayesian calibration and G&R model	Finite Element Analysis	a few cases for demonstration	associated	success demonstration on a few cases
Lee et al. (2018) [26]	prediction of future AAA growth	Machine learning	Non-linear Kernel support vector regression	94 patients	not capable	85% and 71% at 12 and 24 months
Shum et al. (2011) [53]	Classification (ruptured vs unruptured)	Machine learning	J48 decision tree algorithm	76 AAA patients	not capable	classification accuracy of 87%
Parikh et al. (2018) [54]	Classification (elective vs emergent AAA repair)	Machine learning	C5.0 decision tree	150 AAA patients	not capable	classification accuracy of 81%

An alternative approach to make a diameter prediction for future AAA growth in an individual patient is to do a classification via a supervised machine learning technique. Shum et al. [22] developed a model on a retrospective study of 10 ruptured and 66 unruptured aneurysms using a decision tree algorithm and 87% of dataset were correctly classified. Similarly, Parikh et al. built a decision tree based on 150 AAA patients (75 electives and 75 emergent repaired) and demonstrated the classification

accuracy of 81% [23]. They derived similar number of geometrical measurements from 3D constructed of an AAA (n=25 and n=31) as we have (n=21) and provide preferable results. The weakness of these approaches is, however, that they output a binary classification predicting the future state of the AAA as a categorical value rather than a numerical value.

Support Vector Machine (SVM) is a supervised machine learning algorithm which is mostly used for classification problem. However, SVM can also be applied the case of regression and provide flexibility of defining how much error in mm is acceptable in our prediction model. On the other hand, SVM has some major drawbacks against to Bayesian approach. First, SVM has not capable of diameter prediction associated with uncertainty at any given time-point, which is critical for evaluating the aneurysm expansion and surgical planning. Second, the AAA stage of the patients at the time of first scan was not the same so the time of the scan must be shifted in the shared time. Therefore, a customization of SVM requires an iterative approach is not practical in our study to fit a non-linear regression model to the observed scans. Finally, incorporating our prior beliefs such that the average and standard deviation of initial diameters and exponential growth rates are not yielded by SVM to assessment of the aneurysm growth.

The retrospective data set used in this study is geometrical measurements describing the properties of AAA morphology. 118 computed tomography (CT) scans from 26 patients obtained retrospectively at the Seoul National University Hospital were used for this analysis. All AAAs with at least two CT scans and a time interval of at least 6 months were the inclusion criterion. As a result, 106 CT scans from 25 patients (23 men and 2 women) were used. In addition to the morphology of an aneurysm, demographic features of patients such as gender, a history of tobacco use and the comorbidities, especially for, cardiovascular diseases are important in aneurysm growth rate but we do not have such an associated feature. Therefore, these features could not be considered as an exclusion criterion which might be a main factor behind a sudden growth associated high rupture risk and critical in the assessment of aneurysm growth during surveillance. The scans not estimated correctly might be due to having such a commorbidities or medications. Therefore, our next model will attempt to incorporate these clinical factors.

UK Small Aneurysm Trial (UKSAT) [40] showed that the probability of exceeding 55 mm for small aneurysms is less than 1%, and annual, or less frequent, surveillance intervals are safe for all AAAs less than 45 mm. In other studies, the rupture risk for an AAA of 4-4.9 cm-diameter has been estimated to be 0.6-2.1% per year [41]. We also found that aneurysms of 4.5 and 4.9 cm are estimated to reach surgical size in 3 and 2 years, respectively (CI=0.95). This result was supported by the ADAM study, in which 27% of 4-5.5 cm-AAA randomized to the surveillance group had undergone surgical exclusion at 2 years' follow-up [41]. Similarly, AAAs of 4.5-4.9 cm-diameter are expected to reach surgical size in 2-3 years [42].

To avoid the computational inefficiency of a random walk and the requirement to tune the proposal distribution, especially given the high-dimensional target distribution in question, we decided on the Hamiltonian Monte Carlo (HMC) algorithm (or Hybrid Monte Carlo) [20], which is a Markov Chain Monte Carlo method for obtaining a sequence of random samples. We have not reported the complexity of the proposed solution to classify algorithms with respect to their run time or memory space requirements using Big-O notation. The main reason is that the algorithm does not take a very long time and requires a large memory requirement. Additionally, the HMC algorithm is a stochastic algorithm which is run with a pre-determined burn-in and subsequent fixed number of iterations [20].

In a summary, a rapid expansion of AAA, often associated with higher rupture risk, might be observed. This is clinically important for the prognosis of aneurysm growth during surveillance because the required immediate intervention based on the criteria defined by international guidelines might be overlooked. Therefore, the aneurysm growth model was specified according to individual patient characteristics. Additionally, using other geometrical measurements enhanced the exponential growth model. A tool with the improved potential of predicting AAA expansion or assessment of rupture risk, which is important in terms of elective surgical intervention and patient management, was developed.



## CHAPTER 6

### CONCLUSION

The guideline for clinical AAA management based on single maximum diameter criterion has been challenged. An augmented criterion, the maximum diameter  $> 5.5$  cm or annual growth rate  $> 1$  cm/year, has been proposed for surgical intervention. There are various alternative measurements demonstrated in previous studies to evaluate aneurysms over time. Aneurysm volume, for example, is an alternative method proposed by several studies to assess the development of AAA and to evaluate rupture risk. Similarly, the morphology of aneurysms is important for patient monitoring. There is, however, scarcity of morphological studies using longitudinal CT scan images. Therefore, this work aimed to construct a larger database of morphological parameters and to enhance the predictability AAA growth for high-risk aneurysms. A total of 21 measurements of the aneurysm's 3D geometry, reflecting the properties of the aneurysm at the time of the scan, were classified as either primary or secondary and analyzed in terms of their correlations for each observation. In addition, the growth rate for each measurement was calculated in a non-linear fashion and their pairwise correlations were also analyzed.

The exponential growth model was constructed using various diameter measurements, and spherical diameter was found to be the best representative of growth. This measure provides useful information about the evolution of aneurysm size and may be helpful clinically. Nevertheless, there were some major limitations presented in our study: an analytic solution, which is not feasible for calculating the posterior estimates of most non-trivial models, was used and a point estimate without any confidence was provided. Furthermore, because the model was primarily built for reflecting the common characteristics of the population, and since the aneurysm growth over the time does not necessarily follow the common pattern for all patients, each patient having different characteristics, accuracy suffered for patients having relatively faster or slower AAA growth. Finally, the exponential growth model was specified using only a single geometrical measurement, while a number of geometrical measurements together might explain sudden aneurysm growth better.

In this study, a two-system approach based on Bayesian calibration was used and the aneurysm growth model was specified according to individual patient characteristics. The distribution estimates based on a summarization of samples

drawn from the specified model using Markov Chain Monte Carlo (MCMC) samplers. However, only a subset of Korean patients from a single institution was analyzed, thus the results may not be extrapolated to the majority of patients. Therefore, a new set of measurements in a large multicenter study can enhance the prediction capability of the model and contribute the current method of surveillance of patients with a small AAA from clinical aspects. Our next model will attempt to extend the data set by obtaining CTA scans from Turkish population and evaluate the performance of the prediction growth model. Particularly, these findings of the master curve for the spherical diameters for Korean population could be compared to the results obtained for Turkish population.

The prediction model was built specifically on patient characteristics using the various geometrical measurements enhanced the prediction capability of a measurement at any time-point, along with an evaluation of the associated uncertainty. The proposed tool might be helpful clinically, especially for a rapid expansion of AAA, often associated with higher rupture risk, in terms of elective surgical intervention and patient management. This is clinically important for monitoring the prognosis of aneurysm growth during the surveillance because the required immediate intervention based on the criteria defined by international guidelines might be overlooked.

Although, the main motivation behind the study is finding a model, which helps clinicians to effectively manage the prognosis of AAA patients during the surveillance, we also contributed how to construct a 3D model of an AAA sac and measure hemodynamic forces using a number of open source software, which are free and flexible to make research.

## **6.1. Limitation and Future Works**

Although this study has been able to give insight into the screening intervals using longitudinal CTA scans and to provide a tool having the improved potential of predicting AAA expansion or assessment of rupture risk, it has some limitations. First of all, the master curve, established in this study, was based on a purely heuristic approach. Particularly, this study assumed that individual growth patterns are identical to the representative growth pattern, while the maximum diameters of AAA patients at the time of first scan were not identical to other patients. Despite the lack of understanding of the exact biochemical mechanisms, various data-driven or feature-based approaches have proven useful for medical application [28], [43], [69]; this study might provide a new utility for the accurate prediction of AAA growth rate. Second, decision-making related to clinical management for AAA patients is complicated because information of impending AAAs prior to rupture is rarely available or surrogates, for example, AAAs of high rupture risk that is required for immediate intervention can be used [6]. This study does not use ruptured CT scans, and the direct rupture risk assessment is beyond the scope of this study. Third, the AAA growth curve modelled here is only used for the assessment of the likelihood of

an AAA rupture according to the maximum diameter protocols [2], but other factors such as the patient's age, presence of coexistent peripheral artery disease, peripheral aneurysm and whether AAAs are asymptomatic/symptomatic may be important to consider when determining when to proceed with elective AAA repair [6], [7]. Fourth, this is a retrospective and one hospital involved study, in which 106 CT scan images from 25 Korean AAA patients were obtained. The prediction model was specified based on the characteristics of a subset of Korean population. However, the average annual growth rates based on the baseline diameter have large variation [29], because various populations were examined [20]. Therefore, a new set of measurements in a large multicenter study can enhance the prediction capability of the model and contribute the current method of surveillance of patients with a small AAA from clinical aspects. Particularly, these findings of the master curve for the spherical diameters could not be compared to other results in literature. Furthermore, the intra-observer and inter-observer variability in CT measurements is usually  $\pm 5$ mm, so it may take 3 years to recognize an aneurysm with a growth rate of 2 mm/year [12]. Finally, for the purpose of evaluating growth rates in various geometrical measurements, cross sections at different imaging time points were assumed to be at the same centerline position corresponding to each other.

Regardless of these limitations, this study provides valuable information about aneurysm evolution using various geometrical measurements and offers an acceptable growth model for development of an improved surveillance program. Furthermore, a clinical helpful tool for the management of AAA development by considering the patient specific characteristics and various geometrical measurements was provided, and an acceptable growth model for the development of an improved surveillance program was offered, even for AAAs such a sudden growth was observed.





## REFERENCES

- [1] J. S. Lindholt, S. Juul, H. Fasting, and E. W. Henneberg, "Hospital Costs and Benefits of Screening for Abdominal Aortic Aneurysms. Results from a Randomised Population Screening Trial," *Eur. J. Vasc. Endovasc. Surg.*, vol. 23, no. 1, pp. 55–60, Jan. 2002, doi: 10.1053/EJVS.2001.1534.
- [2] K. A. Vardulaki, T. C. Prevost, N. M. Walker, N. E. Day, A. B. M. Wilmink, C. R. G. Quick, H. A. Ashton, R. A. P. Scot, "Growth rates and risk of rupture of abdominal aortic aneurysms," *Br. J. Surg.*, 1998, doi: 10.1046/j.1365-2168.1998.00946.x.
- [3] H. B. B. S. D. Bergqvist, "Incidence and prevalence of abdominal aortic aneurysms, estimated by necropsy studies and population screening by ultrasound.," *Ann N Y Acad Sci*, vol. 800, pp. 1–24, 1996.
- [4] F. A. Lederle, S. E. Wilson, G. R. Johnson, D. B. Reinke, F. N. Littooy, C. W. Acher, ... D. Bandyk, "Design of the abdominal aortic Aneurysm Detection and Management Study. ADAM VA Cooperative Study Group.," *J. Vasc. Surg.*, vol. 20, no. 2, p. 296, 1994.
- [5] A. B. M. Wilmink and C. R. G. Quick, "Epidemiology and potential for prevention of abdominal aortic aneurysm," *Br. J. Surg.*, vol. 85, no. 2, pp. 155–162, 1998, doi: 10.1046/j.1365-2168.1998.00714.x.
- [6] A. T. Hirsch, Z. J. Haskal, N. R. Hertzner, C. W. Bakal, M. A. Creager, ... B. Riegel, "ACC/AHA 2005 practice guidelines for the management of patients with peripheral arterial disease (lower extremity, renal, mesenteric, and abdominal aortic): Executive summary," *Circulation*. 2006, doi: 10.1161/CIRCULATIONAHA.106.173994.
- [7] E. L. Chaiko, D. C. Brewster, R. L. Dalman, M. S. Makaroun, K. A. Illig, G. A. Sicard, ... F. J. Veith, "The care of patients with an abdominal aortic aneurysm: The Society for Vascular Surgery practice guidelines," *J. Vasc. Surg.*, 2009, doi: 10.1016/j.jvs.2009.07.002.
- [8] P. M. Brown, D. T. Zelt, and B. Sobolev, "The risk of rupture in untreated aneurysms: the impact of size, gender, and expansion rate," *J. Vasc. Surg.*, vol. 37, no. 2, pp. 280–284, 2003.
- [9] S. C. Nicholls, J. B. Gardner, M. H. Meissner, and K. H. Johansen, "Rupture in small abdominal aortic aneurysms," *J. Vasc. Surg.*, vol. 28, no. 5, pp. 884–888, Nov. 1998, doi: 10.1016/S0741-5214(98)70065-5.

- [10] J. T. Brown A, Louise C; Powell A, "Risk Factors for Aneurysm Rupture in Patients Kept Under Ultrasound Surveillance," *Ann. Surg.*, vol. 230, no. 3, p. 289, 1999.
- [11] R. C. Darling, C. R. Messina, D. C. Brewster, and L. W. Ottinger, "Autopsy study of unoperated abdominal aortic aneurysms. The case for early resection.," *Circulation*, vol. 56, no. 3 Suppl, 1977.
- [12] R. Limet, N. Sakalihassan, and A. Albert, "Determination of the expansion rate and incidence of rupture of abdominal aortic aneurysms.," *J. Vasc. Surg.*, vol. 14, no. 4, p. 540, 1991.
- [13] P. A. Armstrong; M. R. Back; D. F. Bandyk; A. S. Lopez; S. K. Cannon, "Optimizing compliance, efficiency, and safety during surveillance of small abdominal aortic aneurysms," *J. Vasc. Surg.*, vol. 46, no. 2, pp. 190–196, 2007.
- [14] A. Dugas, É. Therasse, C. Kauffmann, A. Tang, S. Elkouri, A. Nozza, ... G. Soulez, "Reproducibility of abdominal aortic aneurysm diameter measurement and growth evaluation on axial and multiplanar computed tomography reformations," *Cardiovasc. Intervent. Radiol.*, vol. 35, no. 4, pp. 779–787, 2012.
- [15] A. Long, L. Rouet, J. S. Lindholt, and E. Allaire, "Measuring the maximum diameter of native abdominal aortic aneurysms: review and critical analysis," *Eur. J. Vasc. Endovasc. Surg.*, vol. 43, no. 5, pp. 515–524, 2012.
- [16] S. C. Nicholls, J. B. Gardner, M. H. Meissner, and K. H. Johansen, "Rupture in small abdominal aortic aneurysms," *J. Vasc. Surg.*, vol. 28, no. 5, pp. 884–888, 1998.
- [17] F. A. Lederle, S. E. Wilson, G. R. Johnson, D. B. Reinke, F. N. Littooy, C. W. Acher, ... D. Bandyk, "Rupture rate of large abdominal aortic aneurysms in patients refusing or unfit for elective repair," *Jama*, vol. 287, no. 22, pp. 2968–2972, 2002.
- [18] P. M. Brown, D. T. Zelt, B. Sobolev, J. W. Hallett, and Y. Sternbach, "The risk of rupture in untreated aneurysms: The impact of size, gender, and expansion rate," *J. Vasc. Surg.*, 2003, doi: 10.1067/mva.2003.119.
- [19] S. T. Kwon, W. Burek, A. C. Dupay, M. Farsad, S. Baek, E. A. Park, and W. Lee, "Interaction of expanding abdominal aortic aneurysm with surrounding tissue: Retrospective CT image studies," *J Nat Sci*, vol. 1, no. 8, p. e150, 2015.
- [20] J. T. Powell, M. J. Sweeting, L. C. Brown, S. M. Gotensparre, F. G. Fowkes, and S. G. Thompson, "Systematic review and meta-analysis of growth rates of small abdominal aortic aneurysms," *Br. J. Surg.*, vol. 98, no. 5, pp. 609–618, 2011.
- [21] R. O. Forsythe, D. E. Newby, and J. M. J. Robson, "Monitoring the biological

- activity of abdominal aortic aneurysms beyond ultrasound,” *Heart*, vol. 102, no. 11, pp. 817–824, 2016.
- [22] A. Abbas, R. Attia, A. Smith, and M. Waltham, “Can We Predict Abdominal Aortic Aneurysm (AAA) Progression and Rupture by Non-Invasive Imaging? A Systematic Review,” *Int. J. Clin. Med.*, vol. 2, no. 04, p. 484, 2011.
  - [23] R. Lee, A. Jones, I. Cassimjee, and A. Handa, “International opinion on priorities in research for small abdominal aortic aneurysms and the potential path for research to impact clinical management,” *Int. J. Cardiol.*, vol. 245, 2017.
  - [24] M. Farsad, S. Zeinali-Davarani, J. Choi, and S. Baek, “Computational Growth and Remodeling of Abdominal Aortic Aneurysms Constrained by the Spine,” *J. Biomech. Eng.*, vol. 137, no. 9, Sep. 2015, doi: 10.1115/1.4031019.
  - [25] S. Zeinali-Davarani and S. Baek, “Medical image-based simulation of abdominal aortic aneurysm growth,” *Mech. Res. Commun.*, vol. 42, pp. 107–117, 2012, doi: 10.1016/j.mechrescom.2012.01.008.
  - [26] R. Lee, D. Jarchi, R. Perera, A. Jones, I. Cassimjee, A. Handa, ... E. Sideso, “Applied machine learning for the prediction of growth of abdominal aortic aneurysm in humans,” *EJVES short reports*, vol. 39, pp. 24–28, 2018.
  - [27] L. Zhang, Z. Jiang, J. Choi, C. Y. Lim, T. Maiti, and S. Baek, “Patient-Specific Prediction of Abdominal Aortic Aneurysm Expansion using Bayesian Calibration,” *IEEE J. Biomed. Heal. informatics*, 2019.
  - [28] G. Martufi, M. Auer, J. Roy, J. Swedenborg, N. Sakalihasan, G. Panuccio, T. C. Gasser, and T. Christian, “Multidimensional growth measurements of abdominal aortic aneurysms,” *J. Vasc. Surg.*, vol. 58, no. 3, pp. 748–755, 2013.
  - [29] H. Gharahi, B. A. Zambrano, C. Lim, J. Choi, W. Lee, and S. Baek, “On growth measurements of abdominal aortic aneurysms using maximally inscribed spheres,” *Med. Eng. Phys.*, 2015, doi: 10.1016/j.medengphy.2015.04.011.
  - [30] K. Novak, S. Polzer, T. Krivka, R. Vlachovsky, R. Staffa, L. Kubicek, L. Lambert, and J. Bursa, “Correlation between transversal and orthogonal maximal diameters of abdominal aortic aneurysms and alternative rupture risk predictors,” *Comput. Biol. Med.*, vol. 83, no. March, pp. 151–156, 2017, doi: 10.1016/j.combiomed.2017.03.005.
  - [31] R. Limet, N. Sakalihasan, and A. Albert, “Determination of the expansion rate and incidence of rupture of abdominal aortic aneurysms,” *J. Vasc. Surg.*, vol. 14, no. 4, pp. 540–548, Oct. 1991, doi: 10.1016/0741-5214(91)90249-T.
  - [32] Y. G. Wolf, W. S. Thomas, F. J. Brennan, W. G. Goff, M. J. Sise, and E. F. Bernstein, “Computed tomography scanning findings associated with rapid expansion of abdominal aortic aneurysms,” *J. Vasc. Surg.*, vol. 20, no. 4, pp.

- 529–538, Oct. 1994, doi: 10.1016/0741-5214(94)90277-1.
- [33] R. Limet, N. Sakalihassan, and A. Albert, “Determination of the expansion rate and incidence of rupture of abdominal aortic aneurysms,” *J. Vasc. Surg.*, vol. 14, no. 4, pp. 540–548, Oct. 1991, doi: 10.1016/0741-5214(91)90249-T.
  - [34] J. T. Powell, M. J. Sweeting, L. C. Brown, S. M. Gotensparre, F. G. Fowkes, and S. G. Thompson, “Systematic review and meta-analysis of growth rates of small abdominal aortic aneurysms,” *British Journal of Surgery*. 2011, doi: 10.1002/bjs.7465.
  - [35] P. A. Stonebridge, T. Draper, J. Kelman, J. Howlett, P. L. Allan, R. Prescott, and C. V. Ruckley, “Growth rate of infrarenal aortic aneurysms,” *Eur. J. Vasc. Endovasc. Surg.*, 1996, doi: 10.1016/S1078-5884(96)80137-7.
  - [36] A. R. Brady, S. G. Thompson, F. G. R. Fowkes, R. M. Greenhalgh, and J. T. Powell, “Abdominal aortic aneurysm expansion: Risk factors and time intervals for surveillance,” *Circulation*, 2004, doi: 10.1161/01.CIR.0000133279.07468.9F.
  - [37] J. Golledge, J. Muller, D. Coomans, P. J. Walker, and P. E. Norman, “The Small Abdominal Aortic Aneurysm,” *Eur. J. Vasc. Endovasc. Surg.*, vol. 31, no. 3, pp. 237–238, Mar. 2006, doi: 10.1016/J.EJVS.2005.10.032.
  - [38] M. Vega de Céniga, R. Gómez, L. Estallo, N. de la Fuente, B. Vivien, and A. Barba, “Analysis of Expansion Patterns in 4-4.9 cm Abdominal Aortic Aneurysms,” *Ann. Vasc. Surg.*, 2008, doi: 10.1016/j.avsg.2007.07.036.
  - [39] H. Gharahi, B. A. Zambrano, C. Lim, J. Choi, W. Lee, and S. Baek, “On growth measurements of abdominal aortic aneurysms using maximally inscribed spheres,” *Med. Eng. Phys.*, 2015, doi: 10.1016/j.medengphy.2015.04.011.
  - [40] G. Martufi, M. Auer, J. Roy, J. Swedenborg, N. Sakalihasan, G. Panuccio, T. C. Gasser, and T. Christian, “Multidimensional growth measurements of abdominal aortic aneurysms,” *J. Vasc. Surg.*, 2013, doi: 10.1016/j.jvs.2012.11.070.
  - [41] M. Hirose, Y. Hamada, S. Takamiya, “Predicting the growth of aortic aneurysms: a comparison of linear vs exponential models,” *Angiology*, vol. 46, pp. 413–419, 1995.
  - [42] H. T. Abada, M. R. Sapoval, J.-F. Paul, V. De Maertelaer, E. Mousseaux, and J.-C. Gaux, “Aneurysmal sizing after endovascular repair in patients with abdominal aortic aneurysm: interobserver variability of various measurement protocols and its clinical relevance,” *Eur. Radiol.*, vol. 13, no. 12, pp. 2699–2704, 2003.
  - [43] N. Kontopodis, E. Metaxa, M. Gionis, Y. Papaharilaou, and C. V Ioannou, “Discrepancies in determination of abdominal aortic aneurysms maximum

- diameter and growth rate, using axial and orthogonal computed tomography measurements,” *Eur. J. Radiol.*, vol. 82, no. 9, pp. 1398–1403, 2013.
- [44] A. Dugas, É. Therasse, C. Kauffmann, A. Tang, S. Elkouri, A. Nozza, ... G. Soulez, “Reproducibility of abdominal aortic aneurysm diameter measurement and growth evaluation on axial and multiplanar computed tomography reformations,” *Cardiovasc. Intervent. Radiol.*, 2012, doi: 10.1007/s00270-011-0259-y.
  - [45] S. Baum Mueller, T. D. L. Nguyen, R. P. Goetti, M. Lachat, B. Seifert, T. Pfammatter, and T. Frauenfelder, “Maximum diameter measurements of aortic aneurysms on axial CT images after endovascular aneurysm repair: sufficient for follow-up?,” *Cardiovasc. Intervent. Radiol.*, vol. 34, no. 6, pp. 1182–1189, 2011.
  - [46] A. Parr, M. McCann, B. Bradshaw, A. Shahzad, P. Buttner, and J. Golledge, “Thrombus volume is associated with cardiovascular events and aneurysm growth in patients who have abdominal aortic aneurysms,” *J. Vasc. Surg.*, vol. 53, no. 1, pp. 28–35, 2011.
  - [47] K. Lee, R. K. Johnson, Y. Yin, A. Wahle, M. E. Olszewski, T. D. Scholz, and M. Sonka, “Three-dimensional thrombus segmentation in abdominal aortic aneurysms using graph search based on a triangular mesh,” *Comput. Biol. Med.*, vol. 40, no. 3, pp. 271–278, Mar. 2010, doi: 10.1016/J.COMPBIOMED.2009.12.002.
  - [48] C. M. Scotti, A. D. Shkolnik, S. C. Muluk, and E. A. Finol, “Fluid-structure interaction in abdominal aortic aneurysms: effects of asymmetry and wall thickness,” *Biomed. Eng. Online*, vol. 4, no. 1, p. 64, 2005.
  - [49] A. Siika, M. L. Liljeqvist, R. Hultgren, C. Gasser, and J. Roy, “AAA Rupture Often Occurs Outside the Maximal Diameter Region and is Preceded by Rapid Local Growth and an Increased Biomechanical Rupture Risk Index,” *Eur. J. Vasc. Endovasc. Surg.*, vol. 50, no. 3, p. 390, 2015.
  - [50] H. Kurvers, F. J. Veith, E. C. Lipsitz, T. Ohki, N. J. Gargiulo, N. S. Cayne, ... C. Santiago, “Discontinuous, staccato growth of abdominal aortic aneurysms,” *J. Am. Coll. Surg.*, vol. 199, no. 5, pp. 709–715, 2004, doi: 10.1016/j.jamcollsurg.2004.07.031.
  - [51] E. Akkoyun, H. Gharahi, S. T. Kwon, B. A. Zambrano, A. Rao, A. A. Acar, W. Lee, and S. Baek, “Defining master curve of abdominal aortic aneurysm growth and its potential utility of clinical management,” *Manuscr. Submitt. Publ.*, 2019.
  - [52] M. D. Hoffman and A. Gelman, “The No-U-Turn sampler: adaptively setting path lengths in Hamiltonian Monte Carlo,” *J. Mach. Learn. Res.*, vol. 15, no. 1, pp. 1593–1623, 2014.

- [53] J. Shum *et al.*, “Quantitative assessment of abdominal aortic aneurysm geometry,” *Ann. Biomed. Eng.*, vol. 39, no. 1, pp. 277–286, Jan. 2011, doi: 10.1007/s10439-010-0175-3.
- [54] S. A. Parikh, R. Gomez, M. Thirugnanasambandam, S. S. Chauhan, V. De Oliveira, S. C. Muluk, M. K. Eskandari, and E. A. Finol, “Decision Tree Based Classification of Abdominal Aortic Aneurysms Using Geometry Quantification Measures,” *Ann. Biomed. Eng.*, vol. 46, no. 12, pp. 2135–2147, Dec. 2018, doi: 10.1007/s10439-018-02116-w.
- [55] S. T. Kwon, W. Burek, A. C. Dupay, M. Farsad, S. Baek, E. A. Park, and W. Lee, “Interaction of expanding abdominal aortic aneurysm with surrounding tissue: Retrospective CT image studies,” 2015.
- [56] T. B. Glantz, Stanton A and Slinker, Bryan K and Neilands, *Primer of applied regression and analysis of variance*. McGraw-Hill New York, 1990.
- [57] A. Hawkins-Daarud, S. Prudhomme, K. G. van der Zee, and J. T. Oden, “Bayesian calibration, validation, and uncertainty quantification of diffuse interface models of tumor growth,” *J. Math. Biol.*, vol. 67, no. 6–7, pp. 1457–1485, 2013.
- [58] N. Kontopodis, E. Metaxa, M. Gionis, Y. Papaharilaou, and C. V. Ioannou, “Discrepancies in determination of abdominal aortic aneurysms maximum diameter and growth rate, using axial and orthogonal computed tomography measurements,” *Eur. J. Radiol.*, vol. 82, no. 9, pp. 1398–1403, Sep. 2013, doi: 10.1016/J.EJRAD.2013.04.031.
- [59] A. Dugas, É. Therasse, C. Kauffmann, A. Tang, S. Elkouri, A. Nozza, ... G. Soulez, “Reproducibility of abdominal aortic aneurysm diameter measurement and growth evaluation on axial and multiplanar computed tomography reformations,” *Cardiovasc. Intervent. Radiol.*, 2012, doi: 10.1007/s00270-011-0259-y.
- [60] B. A. Zambrano, H. Gharahi, C. Y. Lim, F. A. Jaber, J. Choi, W. Lee, and S. Baek, “Association of Intraluminal Thrombus, Hemodynamic Forces, and Abdominal Aortic Aneurysm Expansion Using Longitudinal CT Images,” *Ann. Biomed. Eng.*, 2016, doi: 10.1007/s10439-015-1461-x.
- [61] A. Parr, M. McCann, B. Bradshaw, A. Shahzad, P. Buttner, and J. Golledge, “Thrombus volume is associated with cardiovascular events and aneurysm growth in patients who have abdominal aortic aneurysms,” *J. Vasc. Surg.*, vol. 53, no. 1, pp. 28–35, Jan. 2011, doi: 10.1016/J.JVS.2010.08.013.
- [62] L. Cappeller, WA and Engelmann, H and Blechschmidt, S and Wild, M and Lauterjung, “Possible objectification of a critical maximum diameter for elective surgery in abdominal aortic aneurysms based on one- and three-dimensional ratios,” *J. Cardiovasc. Surg. (Torino)*, vol. 38, no. 6, p. 623–628,

1997.

- [63] C. M. Scotti, A. D. Shkolnik, S. C. Muluk, and E. A. Finol, “Fluid-structure interaction in abdominal aortic aneurysms: Effects of asymmetry and wall thickness,” *Biomed. Eng. Online*, 2005, doi: 10.1186/1475-925X-4-64.
- [64] B. Sonesson, F. Hansen, H. Stale, and T. Länne, “Compliance and diameter in the human abdominal aorta—the influence of age and sex,” *Eur. J. Vasc. Surg.*, vol. 7, no. 6, pp. 690–697, 1993.
- [65] B. A. Zambrano, H. Gharahi, C. Y. Lim, F. A. Jaber, J. Choi, W. Lee, and S. Baek, “Association of Intraluminal Thrombus, Hemodynamic Forces, and Abdominal Aortic Aneurysm Expansion Using Longitudinal CT Images,” *Ann. Biomed. Eng.*, 2016, doi: 10.1007/s10439-015-1461-x.
- [66] M. Vega de Céniga, R. Gómez, L. Estallo, L. Rodríguez, M. Baquer, and A. Barba, “Growth rate and associated factors in small abdominal aortic aneurysms,” *Eur. J. Vasc. Endovasc. Surg.*, 2006, doi: 10.1016/j.ejvs.2005.10.007.
- [67] T. S. Brady A, Brown L, Fowkes F, Greenhalgh R, Powell J, Ruckley C, “Long-Term Outcomes of Immediate Repair Compared with Surveillance of Small Abdominal Aortic Aneurysms,” *Surv. Anesthesiol.*, 2003, doi: 10.1097/00132586-200306000-00031.
- [68] E. D. Lederle FA, Wilson SE, Johnson GR, Reinke DB, Littooy FN, Acher CW, Ballard DJ, Messina LM, Gordon IL, Chute EP, Krupski WC, Busuttil SJ, Barone GW, Sparks S, Graham LM, Rapp JH, Makaroun MS, Moneta GL, Cambria RA, Makhoul RG, “Immediate repair compared with surveillance of small abdominal aortic aneurysms,” 2002.
- [69] M. Vega de Céniga, R. Gómez, L. Estallo, L. Rodríguez, M. Baquer, and A. Barba, “Growth rate and associated factors in small abdominal aortic aneurysms,” *Eur. J. Vasc. Endovasc. Surg.*, 2006, doi: 10.1016/j.ejvs.2005.10.007.





## APPENDICES

### APPENDIX A

#### A. Patient Specific Blood Flow Simulation and Analyses

The cardiovascular hemodynamic modeling for an AAA using CT scan was not straightforward, even the same guideline prepared for an idealized vessel was followed. In this study, an end-to-end procedure that can be used to construct 3D models of the aneurysm and run hemodynamics simulations with realistic choices for flow parameters and profiles were presented. The steps required for modeling the biomechanical behavior of an AAA were explained. The first part of the section covered the important aspects of the data characteristics. The second part introduced the 2D segmentation using patient data and addressed the encountered issues during the analyses. And the final part explained the 3D segmentation, building a solid model of aneurysm sac, meshing and numerical analysis.

##### 1. The characteristics of data

The input data for the simulation can be categorized under two main groups such as public data (healthy MRI scan) available in literature and patient data (AAA CT scan) in terms of PhD thesis study. The public data is provided by the software developer group (San Diego University) in order to demonstrate how to use the software properly and show the success of the software by visualizing the result. On the other hand, we have both contrast and non-contrast CT images, where the lumen of an abdominal aorta is enhanced using radioactive chemical substance. There are many characteristic differences between patient and public data which are summarized in the following table.

##### *Public Data*

This is a MRI scan, where all the tasks defined by software user guideline can be applicable and the results can be obtained using SimVascular software alone successfully. There is no aneurysm and thrombus (ILT) on the image and the aorta can be easily discriminated just using intensity value from around the other tissues. Therefore, creating a 3D model for a region of interested (ROI) of the aorta (abdominal region) is straightforward using 2D segmentation and lofting properly. The structure of aorta is not complex. For this reason, meshing and applying for finite element analysis can be performed using the guide without any additional task.

Table1. The list of differences between public and patient data

Public Data	Patient Data
MRI scan	CTA scan
Healthy person	Patient with AAA
No thrombus	Large amount of thrombus
Simple structure	Complex structure with high curvature
Easy segmentation using only threshold	Thresholding and shape properties are not sufficient alone to segment
Having high discriminating features	Low discriminating features around the cells
Single modality	Contrast and non-contrast modality with 3.0 and 5.0 cm slice thickness

### ***Patient Data***

There is thrombus throughout the aorta and its structure is complex. It is difficult to segment aorta from around the tissues using only intensity values. Level set algorithm which takes into account the shape of the vessel and intensity value were also not sufficient to segment image in an automatic way. Therefore, manual correction and also medical expertise sometimes required for segmenting many of the slices again. As a result, performing sequential tasks does not work as before and SimVascular platform is not sufficient alone to obtain the results.

Non-contrast image means that no substance is used especially for the lumen enhancement. Therefore, thrombus and lumen intensity values are very close to each other. Additionally, even a contrast image is used, discriminating aorta from the other tissues such as vein are very difficult even with the eyes. Therefore, a fully automatic method to construct 3D solid model is almost impossible. Using ITK-Snap tool to segment aorta (lumen and thrombus together) based on the active contour as before could not be possible. For this reason, a semi-automatic method is preferred for an AAA to segment lumen and thrombus together.

A contrast image (3 cm thickness) having aneurysm with 7.1 cm diameter was demonstrated in Figure 1. The contrast DICOM image has 150 slices throughout the axial plane with 512 rows and 512 columns. This is an example of scans where lumen is enhanced using substance. As a result, the intensity value of lumen throughout the aorta is different from intensity values of all around the tissues. The lumen can be, thus, segmented successfully and automatically.

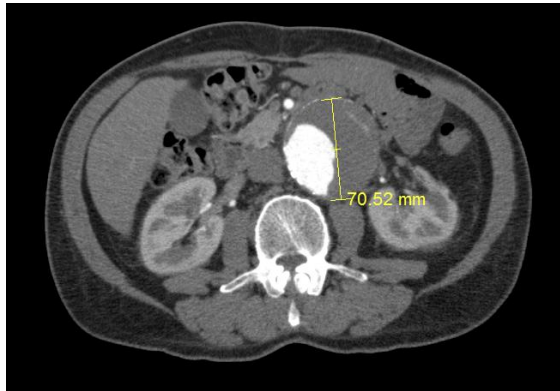


Figure 1. An axial slice from contrasted CTA image

## 2. Building a solid model for an AAA

Visualization and enhancement of patient data using SimVascular is straightforward by adjusting contrast with defining threshold. However, building a cardiovascular solid model is not possible since segmentation on 2D level fails on the many slices. Firstly, SimVascular does not recognize the file format. Therefore, DICOM image series has to be converted into a vti file format on which SimVascular can analyze. There is a library on GNU platform, called `gdcm2vtk`, converts the data to the proper format. Furthermore, determining center line of vessel as a path is the most critical part in 2D segmentation. Moving sphere, a ROI to segment specific slice, throughout the path depends on the path planning. Since the platform could not visualize the image in all the plane, the path could not be determined as a vessel center line. Additionally, the fact that a diameter of a vessel could not be higher than 5 cm and sphere must be perpendicular to slice are assumed. These are some examples of the limitations of the platform that makes very difficult to work for patient data having large aneurysm.

ITK-Snap, an alternative open source platform, mainly designed for segmenting brain image especially for sub-cortex region, where the structure of the tissues is complex. There is a built-in function, based on the active contour algorithm, is used for automatically 3D segment of the lumen throughout the aorta. Firstly, the region of interest is defined using visualization on the coordinate system. To discriminate lumen from the background as a binary image, clustering and thresholding are functionalities that the software provides. Thresholding is a good alternative to get binary image properly, since ITK-Snap provides the status of a segmentation on view screen online, and a responsive environment for various threshold values. After getting the binary image, the various size of bubbles was inserted inside the image throughout the sagittal plane and run the iterative algorithm. How the segmentation goes can be monitored over three planes as well as 3D screen online, where an AAA structure is progressively formed.

The left image in Figure 2 demonstrates an abdominal aortic aneurysm on a sagittal plane for a contrast CT image. It requires to be enhanced in order to visualize the edges

as well as tissue that we are interested better. ITK-Snap provides a contrast adjustment tool where we can get rid of the noisy part of the image. The part of the image where intensity values are too low are set to zero to show meaningful evidence. Thus, the lumen as well as the edge of thrombosis is visualized better. Finally, we need to define RoI (region of interest) on the image because we are especially focusing on the abdominal aortic aneurysms. The right image is a demonstration of defining RoI on the sagittal plane. We need also defines the RoI for coronal and axial planes properly.

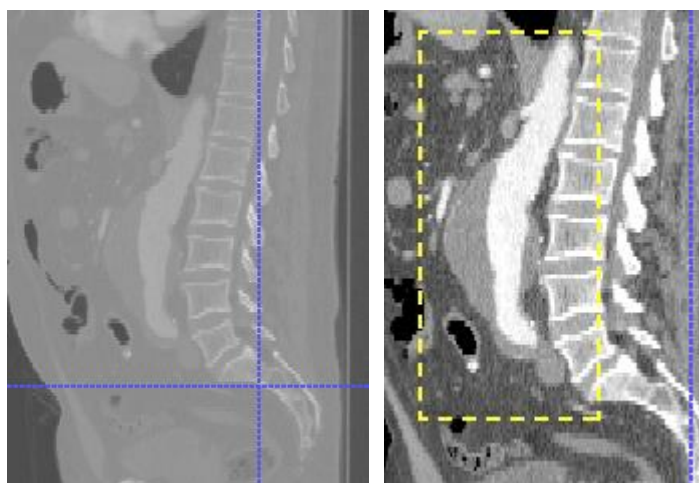


Figure 2. A demonstration of a contrast scans and image enhancement with specified RoI

Active contour is a well-known method that we can segment an image iteratively. Firstly, we need to have a binary image where lumen is foreground and represented as white, and all other part of the tissue is background and represented as black. The left screen on the above figure is not a binary image where only black and white pixels are available. However, it is very close to binary image and ITK-Snap can process it properly. As the middle screen shows, the lumen is satisfactorily segmented. The right figure represents the solid model constructed by the 3D segmentation. It is important to keep in mind here that solid model must be smoothed using like Gaussian in order to have a more realistic surface. Figure 3 demonstrates the process of 3D segmentation using active contour algorithm.

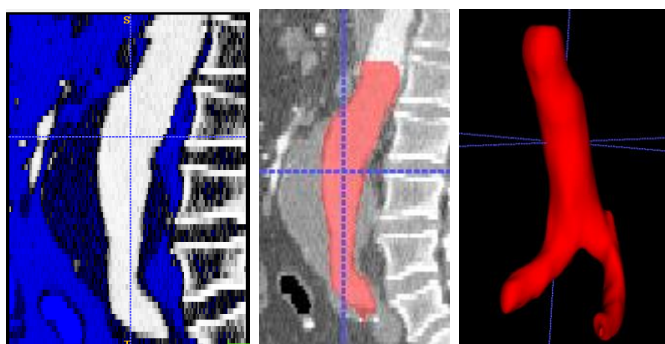


Figure 3. A demonstration of a binary image, a 3D segmentation on a sagittal plane and its solid model

There are many branches of vessels to aorta, which has to be trimmed because no significant effect on the biomechanical behavior observed in the literature. Furthermore, the inlet in where the flow will be prescribed as well as the outlet should be enhanced properly. Otherwise, it would not be possible to identify the boundary conditions such as inlet, outlet and wall. Finally, we need also to perform global operation like fill in the holes, smoothing the surfaces properly.

### **3. Meshing and face identification**

ITK-Snap is a good platform to get solid model for an AAA within the defined region. However, it does not run the simulation for the blood flow analysis. SimVascular can use Navier Stokes equation for the biomechanical modelling of an aorta aneurysm but it requires complete mesh of the model. Therefore, constructed 3D model should be migrated into SimVascular platform where we can define the faces and meshes properly. ITK-Snap is able to export the model in vtp file format which SimVascular can understand. The constructed model should be discretized in order to run numerical analyses properly. Actually, this is a critical step which has a great effect on the accuracy on the obtained result. Therefore, the consecutive steps defined here were followed carefully.

Boundary conditions are also critical for modeling since they accurately capture the physiology of vascular networks outside of the 3D domain of the model. Regardless of the complexities of constructed solid model, each one has three boundary conditions, which are called faces. Unfortunately, the constructed model for a patient has not three faces as expected even of applying preprocessing. Setting angle values in SimVascular determines the number of all faces that solid model has. If the number is kept to small, then tens of faces are represented. Therefore, the angles should be adjusted carefully and the faces might be required to be combined manually. In this example, the number of nodes and elements are 168.157 and 1.002.952, respectively, depend on the tetrahedron size which is 1.1942.

Figure 4 represents the post processing steps after generating meshes. It is possible to increase number of nodes and elements on the bifurcation region of the aorta, where it is critical to capture physical phenomena. SimVascular allows the increase the number of meshes on a specific region using sphere whose radius can be changed properly as the left image represents. The right image demonstrates the increase number of meshes on the layer of wall boundary, where it is important to see the pressure on the surface.

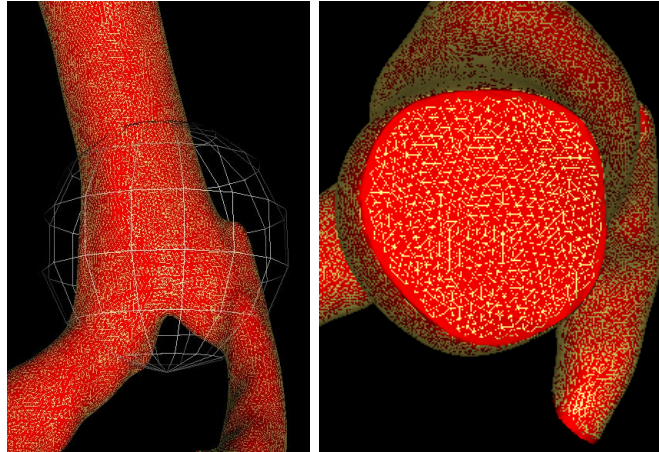


Figure 4. The demonstration of adaptive and boundary meshing

#### 4. Numerical analyses

A number of simulations with various input parameters have been demonstrated on manually created aneurysms, MRI (public data) and CTA (patient data) scan. SimVascular platform was used in order to understand better how it works and what the critical parameters are within the context of cardiovascular modeling for an AAA.

##### Manually created aneurysms

We were manually created simple variations of aneurysms such as fusiform, saccular and no-aneurysms and compared their results obtained for each form of the aneurysms.

There are many parameters affecting the hemodynamic forces especially for evaluating Wall Shear Stress (WSS) (dyne.s/cm<sup>2</sup>), Velocity (cm/s) and Pressure (mmHg), which might play an important role for the rupture. Numbers of time step, flow data, resistance value on the outlet boundary condition, step sequences are just a few of the input parameters, which their effects on the forces was analyzed. The shape of the aneurysm is also critical for the evaluating rupture risk. Therefore, the effect of the shape and the input parameters were both investigated by changing the values and shapes systematically and monitored the results on the time series.

The number of time step, which describes how many iterations will be performed during the simulation kept small as much as possible since high number of iterations require a lot of computation power that takes several hours. It is enough to set about 150 iterations in a simulation for testing purposes. Thus, it would be applicable to run a simulation on a regular PC within an hour. Another important issue is to monitor the residual errors during the simulation in real time. As the guide highlighted, the residual error must be less than 0.01. Therefore, we can also handle how the numerical solution converges for each iteration.

To understand better the simulation parameters, we run tens of simulations and investigated their results. Table 2. shows the fundamentals input parameters, which are required to set for a simulation.

Table 2. Fundamental input parameters necessary to be set

Analytic Shape of Profile	parabolic
Flow Rate File	0.0 -100, 0.2 -100
# of periods	1
# pts in period	2
# fourier modes	1
Outlet BC	zero_pressure_vtp
Wall BC	noslip_vtp
# of time step	150
Time step size	0,004
Resistance Values	16000 16000
Step Sequence	0 1 0 1

Figure 5 visualizes hemodynamic forces after running numerical analyses on manually created simple aneurysms such as fusiform, saccular and no-aneurysms. The viscosity, density and period were set 0.04 poise, 1.06 gr/cm<sup>3</sup> and 0.2 sec for all simulation, respectively. We found from the simulation is that the flows prescribed to inlet is increased, the value of output parameters increased. WSS values are observed higher at saccular form than fusiform. The saccular form of the aneurysms might be critical, because the risk of rupture is relatively higher than fusiform. The diameter of aneurysms has a positive effect on the WSS.

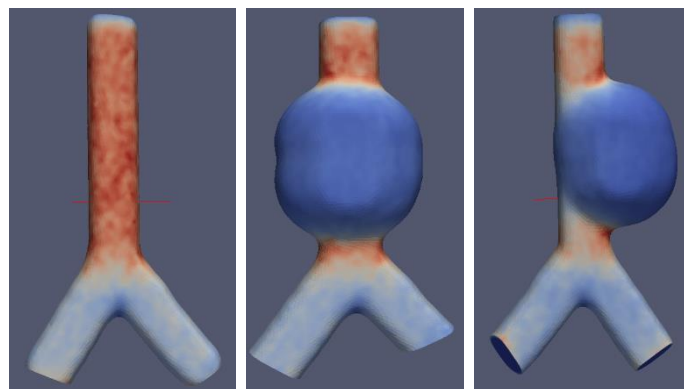


Figure 5. The various forms of aneurysms, no aneurysm (healthy), fusiform and saccular, from left to the right

## Public Data

An MRI scan, public data, was used in this part of the study to understand better how the input parameters affect hemodynamic forces by comparing results obtained for each input parameter. The first set of input parameters (Run #1) was obtained from official guideline published by SimVascular platform, because we wanted to verify our measurements by comparing the references ones. Then, we changed the input parameters systematically and evaluated the hemodynamics forces for each run. Meanwhile, we analyzed the residual error for each simulation and discarded Run #4, because the solution does not converge over the iterations (residual error is higher than 0,01).

The left picture in Figure 6 was provided by the software, while the right one is obtained after our simulation. The right solid model, a specific part of the left one, was constructed by cutting of the iliac at some points to see how the vessel long affects the hemodynamic forces. We found that WSS were almost identical in both examples, when the value of parameters was kept the same. The result shows that the results do not depend on the vessel long in case of keeping the shape the same.

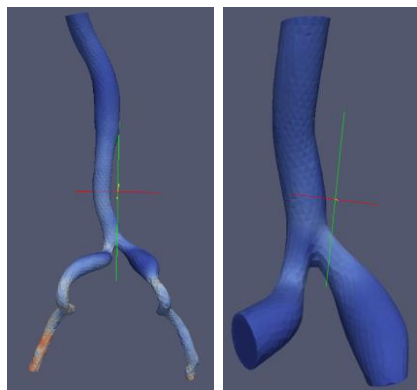


Figure 6. The WSS representation of the aorta after simulations

## Patient Data

In this part of the study, we run the simulations using the patient data. The aim is to understand whether there is a meaningful difference between patients who have various morphology of aneurysms in terms of WSS, velocity and pressure. Therefore, we obtained samples of CTA scans for different patients and run the analyses. We kept the value of input parameters the same for all the simulations and collected results into a file. The hemodynamic forces calculated for each patient.

We found that the pressure values are the identical for all patients having various shape of the aneurysms and the size of a diameter. This result is expected since the pressure is just depend on the resistance and flow rate within the context of resistance boundary condition, which is the basic assumption for the biomechanical modeling. Second, there are tiny changes observed on the values of WSS and velocity obtained for each group. This is not expected, because the shape of the aneurysms is completely different. The velocity, for example, was measured less than 10 cm/sec, while it should



be around 150 cm/sec for a healthy person. Figure 7 demonstrates the flow profile throughout the aneurysm sac.

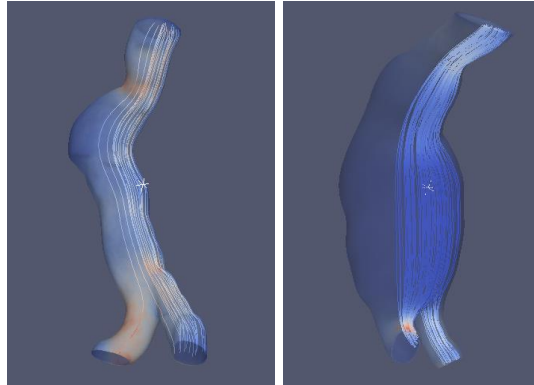


Figure 7. The WSS and velocity distribution for Run 1 (ruptured) and Run 2 (un-ruptured)

To run a simulation using patient data requires a lot of sequential steps and we need to use various software for each step. For example, ITK-Snap is one of the tools that we used for constructing 3D model of an AAA. Then, the model was exported into SimVascular and a number of preprocessing like Gaussian smoothing and face extraction was performed here. We realized that ITK-Snap exports the model in millimeter unit, while SimVascular accepts it in centimeter unit. This was a critical because we run the simulation for aneurysms, where the diameters are around 60-70 cm. Therefore, the WSS as well as velocity values reported in the previous section was too small that we could not extract any meaningful information about the biomechanical model. All the simulations that we run are based on the tetrahedron meshing within Tetgen provided by SimVascular. Before exporting the model into SimVascular, we can also use Paraview in order to remove a number of tetrahedron, which might have a negative effect on the result.

Open flipper is a new tool that we used during the simulation because it has a capability of the scale aneurysm by 0.1. Thus, it would be possible to overcome the issue caused by the unit problem. Furthermore, it also provides smoothing and remeshing to get better result at the final step. Figure 8 demonstrates the flows, form of tribulations, which were not observed in the previous set of runs.

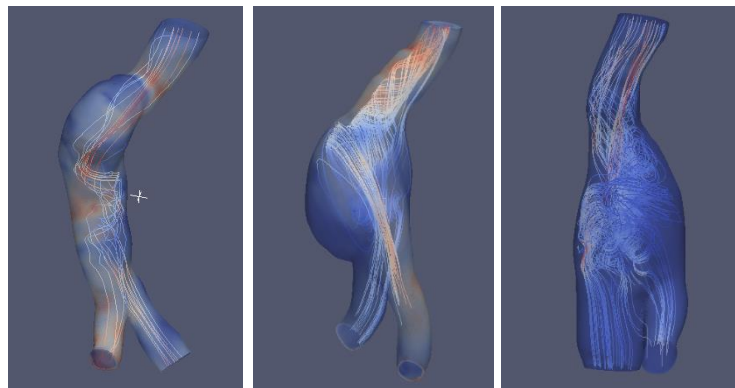


Figure 8. Visualization of WSS and velocity values on the aneurysm

The maximum pressure value was not changed over the patients, because the flow rate and resistance values were the same. However, a pressure whose direction is negative to flow was observed and its value changed among the patients, because the characteristic of flow seems to be a tribulation form.

## 5. Verification of blood flow simulations

The pulsatile flow reflects the real cardiovascular phenomena better. Figure 9 demonstrates a pulsatile flow profile, prepared for a single cardiac cycle where systolic and diastolic are visible. There are two hundred time points defined in the profile file, whereas it was only two in the steady flow.

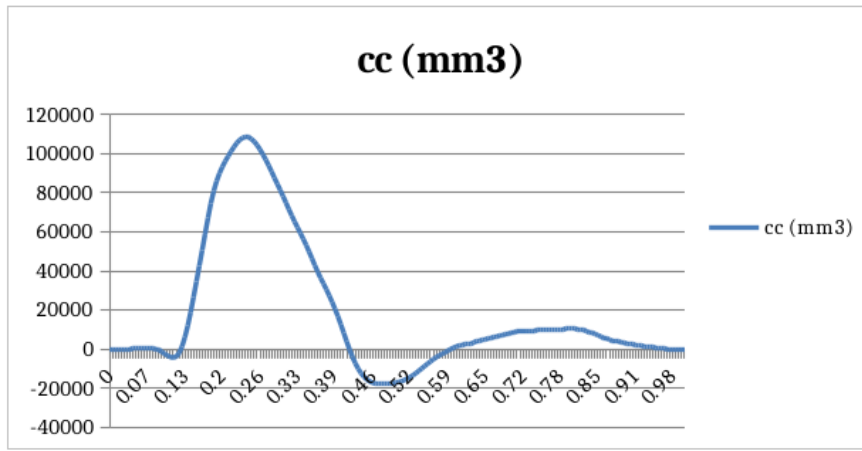


Figure 9. Pulsatile flow prescribed into aorta inlet

The velocity of flow according to various time point during a single cardiac cycle can be visualized. For example, high amount of flow prescribed into aorta at around 0.02, and low amount flow prescribed into aorta at around 0.2 according to pulsatile flow. The velocity was measured respectively to the flow strength at that time; the maximum velocities were 4 mm/s to 765 mm/s, respectively. This was a parabolic flow, where the velocity was zero at the wall and maximum at the center of the aorta, as formulated below.

$$V_z^{max} = \frac{2Q}{\pi r^2}$$

Where  $V_z^{max}$  defines the maximum velocity (mm/s) on the z direction,  $Q$  defines the flow rate (cc) at a specific time point. If we select as a specific time point like  $t=0.2$ , then we can find the flow rate inside the pulsatile flow. The flow rate is 96149 cc at that point. However, it is not an exact value, because we defined Fourier mode in pre-solver file, which makes smooth the flow profile. The diameter is a specific to patient aorta. Therefore, it varies from patient to patient. In this example, we can find the diameter using ParaView by looking at the x and y information. We find out the velocity is around 300 mm/s theoretically, while it is around 400 mm/s computationally in ParaView.

The cut orthogonal to screen is critical for evaluating the hemodynamic forces, as the blood flows throughout the center of the vessel. Otherwise, there is a flow against to wall, which might create some artifacts on the result. When we are opening the file generated by simulation, it shows the minimum and maximum value of the whole part that is an indicator for our prediction. However, there are sometimes the highest or lowest value can be observed close to right and left iliac outlets, which is not belong to aneurysm sac and out of scope in this study.

Even the structure of any aorta is different in terms of diameters of the right and left iliac, the amount of the flow should be the same since the body manages it perfectly. Therefore, it's a good idea to compare the amount of flows over the cardiac cycle time towards to both iliac. Figure 10 shows the amount of flow inside the inlet and outside the both iliac over time. The amount of flow prescribed into inlet is the same the amount of total flow prescribed to outlets, as expected. Furthermore, as the figure shows there is a tiny difference in terms of the amount of flow between right and left iliac, which were ignored in this study. It is possible to make the amount of flow identical for both iliac in case of changing the boundary condition as RCR rather than Resistance. However, it costs additional controlling the simulation and much more computational power. On the other hand, running the simulation for a single cardiac cycle is not enough to getting meaningful results. Even the flow profile seems to be the same between two cardiac cycles; there might be still some differences at the systolic phase during a cardiac cycle. Therefore, the simulations were run at least for 3 or 4 cardiac cycles and the results of the last cycle were analyzed.

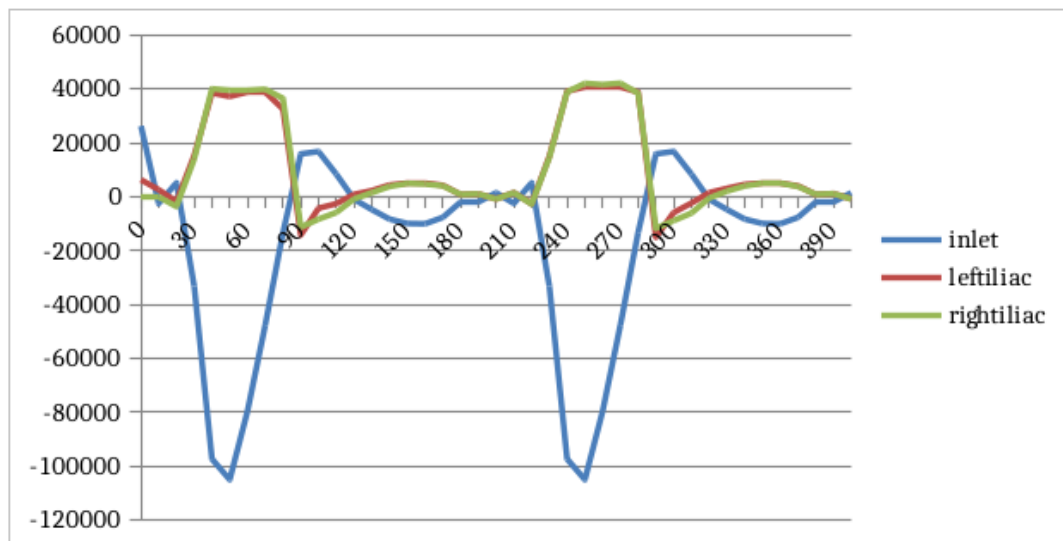


Figure 10. The flow prescribed inlet and outlet respectively

To run a simulation, we need to set initial pressure ( $1180 \text{ dyne/mm}^2$ ) and resistance ( $0.0072 \text{ dyne.s/mm}^5$ ) values for both iliac. Actually, this was a manual adjustment after running the simulations tens of times. In the basic assumption, we should have pressure between 11000 and 17000 Pascal on the outlet. Although, it is not possible to find the pressure on the outlet at the specific time over a cardiac cycle, we can make some assumption as following.

We selected an average amount of flow as 50.000 cc/s at any t time, where the initial pressure is 1180 dyne/mm<sup>2</sup> and the resistance value is 0.0072 dyne.s/mm<sup>5</sup>.

$$p = p_0 + Q \cdot R$$

where  $Q$  is flow rate,  $R$  is resistance and  $p_0$  is initial pressure (recall that 1.0 mmHg = 1333,2 dyne/cm<sup>2</sup> and 1 Pascal = 10 dyne/cm<sup>2</sup>).

$$p = 1180 \text{ dyn/mm}^2 + 50000 \text{ mm}^3/\text{s} \cdot 0.0072 \text{ dyn.s/mm}^5$$

$$p = 1540 \text{ dyn/mm}^2$$

$$p = 15400 \text{ Pascal}$$

The pressure on the outlet is in the range of the reference value, between 10000 and 17000 Pascal. Thus, the initial pressure and resistance values can be optimized using the aforementioned formula.

## 6. Conclusion

Biomechanical behavior of the aneurysm was analyzed within the context of hemodynamic forces to better understand the reasons for gradual aneurysm growth and potential rupture. An end-to-end procedure using various open source software to construct a 3D model of the aneurysm and run hemodynamics simulation were demonstrated.

## APPENDIX B

### B. Instructions for creating a solid model using MIMIC

A 3D model of an AAA was constructed using open source software called ITK-Snap, a strong platform for image segmentation, smoothing the model and exporting the results into SimVascular properly. There is an alternative commercial solution, Mimics. Even there is a community version available; it has lack of functionalities, which are required to construct a 3D model of AAA properly. The instructions for getting a solid model using MIMICS are listed below.

- New project wizard (Open DCM image series and convert)
- Image Enhancement
  - Adjust contrast just for the comfort
  - Thresholding (select Bone and apply)
- Crop Mask (define the RoI)
- Calculate 3D
  - All 3D model of tissues inside the RoI can be observed
- Start region growing
  - Pick up the location of lumen area
  - Calculate 3D
  - Make invisible the previous 3D construction
    - In case of connection between spine and aorta existence, remove it (edit mask and erase using circle)
- Improvements
  - Fill in the gap
  - Remove sharp area and calcification (using edit mask)
  - Calculate 3D again
- Smoothing
  - Right click on the model and select smoothing
  - Iterations between 10 – 15
  - Make correction if required
- Full Functionality is required from that point
  - Wrapping
    - Right click on 3D structures and wrap it in order to fill small gaps
  - Finding the centerline of 3D model
    - Make transparent 3D in order to find normal orthogonal
  - Cut orthogonal to screen
- Export STL file

All the steps listed above can also be done using ITK-Snap but it is not easy as much as Mimics since it has already well defined threshold for lumen and function for

constructing 3D model. However, Mimics is not a must in the study and our university does not have proper license to use full functionality. ITK-Snap with open flipper can also do similar tasks even the usage is a bit more difficult.

## CURRICULUM VITAE

### PERSONAL INFORMATION

Surname, Name : Akkoyun, Emrah  
Nationality : Turkish (TC)  
Date and Place of Birth : 15 November 1985, Ankara  
E-mail : [emrah.akkoyun@metu.edu.tr](mailto:emrah.akkoyun@metu.edu.tr)  
Address : Erzurum Kongresi Cd. Metrokent Sitesi NO:1B/98  
Etimesgut Ankara/TURKEY

### EDUCATION

Degree	Institution	Year of Graduation
MS	METU, Graduate School of Informatics	2011
BS	Dokuz Eylul U., Computer Engineering	2007

### WORK EXPERIENCE

Year	Place	Enrollment
2006-Present	TUBITAK ULAKBIM	Researcher
2016,2017	Michigan State University	Visitor Scholar

### FOREIGN LANGUAGES

Advanced English, Fluent German

### PUBLICATIONS

1. Akkoyun, E., Kwon, S. T., Acar, A. C., Lee, W., & Baek, S. (2020). Predicting abdominal aortic aneurysm growth using patient-oriented growth models with two-step Bayesian inference. *Computers in Biology and Medicine*, 103620.
2. Emrah Akkoyun, Aybar Can Acar, Byron Zambrano and Seungik Baek Cardiovascular Modelling for Abdominal Aortic Aneurysms, 10TH INTERNATIONAL SYMPOSIUM ON HEALTH INFORMATICS AND BIOINFORMATICS (HIBIT 2017), Northern Cyprus, 28-30 June, 2017
3. Akkoyun, E., & Can, T. (2011, July). Parallelization of the functional flow algorithm for prediction of protein function using protein-protein interaction networks. In *2011 International Conference on High Performance Computing & Simulation* (pp. 56-62). IEEE.

4. Ciftcioglu, M. U., Akkoyun, E., & Gokcay, D. (2009, May). Improvement of segmentation in sub-cortical area in MR images of the brain. In 2009 14th National Biomedical Engineering Meeting (pp. 1-4). IEEE.